GLIA

WILEY

Check for updates

RESEARCH ARTICLE

Repetitive injury and absence of monocytes promote astrocyte self-renewal and neurological recovery

Luisa Lange Canhos[1,2,3] | Muxin Chen[1] | Sven Falk[1,2] | Bastian Popper[4] | Tobias Straub[5] | Magdalena Götz[1,2,6] | Swetlana Sirko[1,2]

[1]Physiological Genomics, Biomedical Center, Ludwig-Maximilians-University Munich, Munich, Germany

[2]Institute of Stem Cell Research, Helmholtz Zentrum Munich, Neuherberg, Germany

[3]Graduate School of Systemic Neurosciences (GSN-LMU), Ludwig-Maximilians-University Munich, Munich, Germany

[4]Core Facility Animal Models, Biomedical Center, Ludwig-Maximilians-University Munich, Munich, Germany

[5]Core Facility Bioinformatics, Biomedical Center, Ludwig-Maximilians-University Munich, Munich, Germany

[6]Excellence Cluster for Systems Neurology (SyNergy), Munich, Germany

Correspondence
Magdalena Götz and Swetlana Sirko, Physiological Genomics, Biomedical Center, LMU, Munich, Germany.
Email: magdalena.goetz@helmholtz-muenchen.de (M. G.) and swetlana.sirko@med.uni-muenchen.de (S. S.)

Present address
Sven Falk, Institute of Biochemistry, Emil-Fischer-Center, Friedrich-Alexander-Universität Erlangen-Nürnberg, Erlangen, Germany

Funding information
Deutsche Forschungsgemeinschaft, Grant/Award Number: SFB870; Priority Program 1757 and the Micronet grant within the ERA-Net NEURON program, Grant/Award Number: FKZ: 01EW1705B; Synergy Excellence Cluster and the Priority Program, Grant/Award Number: 1757
Open access funding enabled and organized by Projekt DEAL.

Abstract

Unlike microglia and NG2 glia, astrocytes are incapable of migrating to sites of injury in the posttraumatic cerebral cortex, instead relying on proliferation to replenish their numbers and distribution in the affected region. However, neither the spectrum of their proliferative repertoire nor their postinjury distribution has been examined in vivo. Using a combination of different thymidine analogs and clonal analysis in a model of repetitive traumatic brain injury, we show for the first time that astrocytes that are quiescent following an initial injury can be coerced to proliferate after a repeated insult in the cerebral cortex grey matter. Interestingly, this process is promoted by invasion of monocytes to the injury site, as their genetic ablation (using $CCR2^{-/-}$ mice) increased the number of repetitively dividing astrocytes at the expense of newly proliferating astrocytes in repeatedly injured parenchyma. These differences profoundly affected both the distribution of astrocytes and recovery period for posttraumatic behavior deficits suggesting key roles of astrocyte self-renewal in brain repair after injury.

KEYWORDS

astrocyte topology, cognitive disfunction, inflammation, reactive gliosis, self-renew, TBI

1 | INTRODUCTION

Astrocytes are key for brain function (Chai et al., 2017; Jahn, Scheller, & Kirchhoff, 2015; Oberheim, Goldman, & Nedergaard, 2012), providing metabolic support for neurons and regulating synapse function and plasticity at various levels (Araque et al., 2014; Ben Haim & Rowitch, 2017; Dallerac & Rouach, 2016; Verkhratsky & Nedergaard, 2016). In order to perform these functions, astrocytes must cover the entire parenchyma and tiling mechanisms have been suggested to ensure equal coverage by the fine astrocyte processes

(Hol & Pekny, 2015; Verkhratsky & Nedergaard, 2016; Wilhelmsson et al., 2019). Despite the importance of astrocyte coverage, very little is known about this after brain injury. It has been suggested that after traumatic brain injury (TBI), reactive astrocyte processes overlap and tiling is lost (Pekny & Pekna, 2016; Pekny, Wilhelmsson, Tatlisumak, & Pekna, 2019; Verkhratsky, Rodriguez, & Parpura, 2014), but little is known if and how astrocyte numbers and distribution are recovered.

Studies using GFAP-immunostaining have outlined astrocytes to be enriched around the injured site forming the scar (Anderson et al., 2016; Wanner et al., 2013). However, we have recently shown a disconnect between astrocyte proliferation and the persisting GFAP scar in the CCR2$^{-/-}$ mouse line lacking monocyte invasion (Frik et al., 2018). In this model, astrocyte proliferation was increased, leading to the increased generation of astrocytes, but the accumulation of GFAP-immunoreactivity and other parameters of scar formation were significantly reduced (Frik et al., 2018). These observations prompted us to examine the post-injury distribution of astrocytes, both in WT and CCR2$^{-/-}$ mice.

After an acute insult, astrocytes die, thus becoming reduced in number (Frik et al., 2018; Heimann et al., 2017; Sirko et al., 2015; Zhao, Ahram, Berman, Muizelaar, & Lyeth, 2003). To recover astrocyte numbers at the site of injury, astrocytes could in principle— (a) migrate from other less affected sites (which would lead to an astrocyte depletion there), (b) proliferate (which would restore astrocyte numbers, but may lead to altered distribution if it is not accompanied by migration) and/or (c) differentiate from other progenitor sources, such as NG2 glia (Faiz et al., 2015; Hirrlinger et al., 2009; Nishiyama, Boshans, Goncalves, Wegrzyn, & Patel, 2016; Tripathi, Rivers, Young, Jamen, & Richardson, 2010). Live in vivo imaging revealed the absence of astrocyte migration to the TBI site in the cerebral cortex grey matter (GM) and genetic fate mapping showed limited contribution of other progenitors to the astrocyte pool in this brain region (Bardehle et al., 2013; Buffo et al., 2008; Dimou, Simon, Kirchhoff, Takebayashi, & Gotz, 2008; Komitova, Zhu, Serwanski, & Nishiyama, 2009; Simon, Gotz, & Dimou, 2011; Zawadzka et al., 2010). Thus, astrocyte proliferation could be the main factor determining their postinjury number and distribution. Astrocyte proliferation, is however, limited. Consistent with this, live in vivo imaging showed that only two daughter cells were generated from dividing astrocytes and that astrocyte proliferation occurs predominantly at the vascular niche (Bardehle et al., 2013; Frik et al., 2018). This would predict a disbalance in astrocyte distribution with supposedly increased numbers at the blood vessels (BVs). As this bias of astrocyte proliferation at the vascular niche was also maintained in CCR2$^{-/-}$ mice, where astrocyte proliferation was increased (Frik et al., 2018), this would suggest an even greater disbalance in astrocyte distribution after injury. Here, we examined if this is the case and also determined the neurological outcome by behavioral analysis.

Importantly, astrocyte distribution will also be different depending on the type of astrocyte proliferation. In case only certain subtypes of astrocytes proliferate this may lead to an uneven astrocyte distribution. However, it is not known if after a second insult astrocytes may continue proliferating, or if other astrocytes are recruited. The latter point would be consistent with a model in which many if not most astrocytes can resume proliferation depending on the strength and localization of the pathological stimulus. Conversely, the former proliferation mode restricted to specialized subtypes may result in an even larger dys-balance of astrocyte distribution post injury. Here, we used repetitive cortical injuries and monitored both astrocyte distribution and proliferation after the first and the second injury episodes by different DNA-base analogs, in addition to assessing the neurological outcomes of these mice to formulate hypotheses about beneficial or adverse effects of alterations in astrocyte distribution after brain insults.

2 | MATERIALS AND METHODS

2.1 | Experimental animals

Adult mice (females and males, 2–3 months old) from the following lines were used: C57Bl6/JRj (Janvier labs, France) (referred to as WT), Tg(Aldh1L1-eGFP)OFC789Gsat mice in which enhanced green fluorescent protein (eGFP) is driven by the aldehyde dehydrogenase 1 family member L1 (Heintz, 2004) (referred to as Aldh1L1-GFP), homozygous knock-in CCR2$^{RFP/RFP}$ mice (Saederup et al., 2010) that result in a full knockout of the CCR2 gene (and therefore referred to as CCR2$^{-/-}$), and double transgenic mice obtained from crosses between GLAST^{CreERT2} mice (Mori et al., 2006) and R26R-Confetti mice (Bardehle et al., 2013; Snippert et al., 2010) (referred to as GLAST/Confetti). GLAST/Confetti mice received a total of 3 intraperitoneal (i.p.) injections of 80 µg tamoxifen per gram of body weight (stock solution: 20 mg/ml tamoxifen in corn oil with 10% ethanol) which were delivered every other day within the period of 5 days. The first stab wound (SW) injury was performed 7 days after the last tamoxifen injection. All mice were kept under specified pathogen-free conditions and housed in groups of 2–3 animals in filter top cages and a 12 hr/12 hr light/dark cycle. Mice had free access to water (acidified and desalinated) and standard rodent chow (Altromin, 1310 M). All experimental procedures were performed in accordance with animal welfare policies and approved by the Government of Upper Bavaria.

2.2 | Surgical procedure

Mice were anesthetized with an i.p. injection of midazolam (5 mg/kg of body weight), medetomidine (0.5 mg/kg) and fentanyl (0.05 mg/kg). For local anesthesia, lidocain gel 2% was applied on the skull. A unilateral craniotomy was performed between bregma and lambda cranial sutures to expose the surface of the brain. SW were inflicted by inserting a lancet-shaped knife into the somatosensory cortex gray matter (GM) at the following coordinates: related to bregma +2.0 mm mediolateral, −0.8 to −2.0 mm anteroposterior, and from the surface of the brain −0.6 mm dorsoventral. Afterwards, the skin was sutured and anesthesia was antagonized with a subcutaneous (s.c.) injection of

atipamezol (2.5 mg/kg), flumazenil (0.5 mg/kg), and naloxone (1.2 mg/kg). Meloxicam (1 mg/kg) was administered as a postoperative analgesic for 3 days following surgery. The repetitive SW was performed 14 days after the first one and at the same size and location which was achieved by following the coordinates and by using recorded information of blood vessels as landmarks to assist on recognizing precisely the injury site.

2.3 | BrdU and EdU labeling

For labeling of proliferating cells in vivo, 5-bromo-2′-deoxyuridine or BrdU (Sigma) and 5-ethynyl-2′-deoxyuridine or EdU (Thermo Fisher) were administered via sterilized drinking water (1 mg/ml BrdU or 0.2 mg/ml EdU, 1% sucrose). The BrdU-containing water was administered for the first 10 days after first SW, followed by a 4-day washout period in which animals received regular water, and lastly by a 10-day administration of EdU-containing water. In addition, we ensured that the sequence of application (EdU first/BrdU first) were not different, that both analogues have similar detection sensitivities, and the total number of labeled cells was equal if BrdU was followed by EdU, or BrdU was applied 2x (see Figures S1 and S3).

2.4 | Immunohistochemistry

For immunohistochemistry, mice were anesthetized (i.p. injection of ketamine 100 mg/ml and 2% xylazin, at 0.01 ml/g body weight) and then transcardially perfused with ice-cold phosphate-buffered saline (PBS) for 20 min, followed by 4% paraformaldehyde (PFA) in PBS for 20 min. Brains from wild type (WT), Aldh1L1-GFP and CCR2$^{-/-}$ mice were postfixed in 4% PFA for 2 hr, cryoprotected (30% sucrose in PBS) overnight and then sectioned with the cryostat in 40 μm thick coronal slices. GLAST/Confetti mice brains were postfixed in 4% PFA overnight, embedded in 4% agarose blocks and sectioned in 60 μm thick coronal slices on the vibratome. Sections were incubated in PBS containing 0.5% TritonX-100 (Sigma) and 10% normal goat serum (Thermo Fisher) for 1 hr at room temperature (RT). EdU detection was performed with the Click-iT Edu Alexa Fluor 647 Imaging Kit (Thermo Fisher, C10340) according manufacturer instruction. Immunohistochemistry was carried out using the following primary antibodies: anti GFAP (rabbit, 1:250, Dako, Z0334), anti GFP (chick 1:400, Aves Labs, GFP-1020), anti Sox9 (guinea pig, 1:1500, generously provided by Palle Serup, Copenhagen University, Denmark), anti NeuN (mouse, 1:100, Millipore, MAB377), anti Aldh1L1 (mouse, 1:200, Millipore, MABN495), anti CD31 (rat, 1:100, BD Biosciences, 550274), anti RFP (rabbit, 1:500, Rockland, 600-401-379) overnight at 4°C. After the wash steps with PBS, sections were incubated with species- and subclass-specific secondary antibodies conjugated to Alexa Fluor 488 or 555 (Thermo Fisher) or Cy3 (Dianova) used at 1:500 and incubated for 3 hr at RT. For followed BrdU immunohistochemistry, sections were fixed with 4% PFA for 10 min, washed and underwent treatment with 2 N HCl for 30 min. Afterwards, sections were incubated in sodium tetraborate buffer 0.1 M in PBS (pH 8.5) for 30 min and washed in PBS.

Immunohistochemistry with primary antibody to BrdU (1:200, mouse IgG$_1$, clone BU33, Sigma, B2531) and secondary antibody to mouse IgG$_1$ Alexa Fluor 555 (1:500, Thermo Fisher) was performed as described above. For clonal analysis in GLAST/Confetti mice, both BrdU and EdU were detected with BrdU antibody (1:200, rat, clone BU1/75, Biozol, BZL20630) on sections that underwent acid treatment with 0.01 sodium citrate (pH 6.0) for 20 min at 96°C. After incubation with the primary antibody, secondary antibody to rat Alexa Fluor 647 (1:500, Thermo Fisher) was used. All sections were incubated for 15 min with DAPI (1:1000, Sigma, D9542) for nuclear labeling and mounted on glass slides with Aqua-Poly/Mount (Polysciences). Images were acquired using a laser-scanning confocal microscope (Zeiss, LSM 710), and analyzed with ImageJ 1.49g software. Cell counting was performed with the Cell Counter plug-in for ImageJ 1.49g, by careful inspection across serial optical sections (spaced at 1.5 μm) of confocal Z-stacks acquired with a ×25 objective (NA 0.8). Image processing was performed with ImageJ and Adobe Illustrator CS6 (Adobe Systems) was used for preparation of multipanel figures.

2.5 | Clonal analysis

In order to define multicellular clones generated by single recombined (GFP$^+$ or RFP$^+$) astrocytes in the GLAST/Confetti mice, a threshold for the maximum distance between the single cells in a given clone was established. For this, the minimum distance between two BrdU/EdU-positive cells with different fluorescent protein expression (referred to as "false positive clones") was measured (see Figure S4). In all sections, which contained such "false positive clones" in the injured cerebral cortex GM, the distance between two proliferating cells having a different fluorescent protein was more than 20 μm. Due to the sufficiently sparse recombination rate in many sections (25% in single injury group and 40% in repetitive injuries group) there were no two proliferating cells expressing different fluorescent proteins in the same section. For clone definition, we took a conservative approach and determined the threshold at a 5 μm maximum distance between two cell somatas, as live in vivo imaging showed that astrocytes stay very close to each other following division (Bardehle et al., 2013).

2.6 | Distribution analysis of Sox9-positive cells

Confocal stacks of 40 μm brain sections were acquired on a Zeiss LSM 710 laser scanning microscope. For quantifications, 3–5 multichannel confocal 3D z-stack images per animal from each experimental group and 3–5 animals per group depicted in density plots were maximum projected using Fiji (v2.0.0). In order to get quantifiable binary pictures, the channels for CD31 and Sox9 were subjected to thresholding independently of each other using the Fiji inbuild "Treshold" function. Using the "Analyze Particles" function of Fiji the exact XY coordinates of each Sox9$^+$ cell, as well as of all CD31 positive pixels, were determined. The minimum distance of each Sox9$^+$ cells to the closest blood vessel, as well as to the injury site, was

determined using R (v3.5.0) and RStudio (1.1.453), in particular the "rdist" function contained in the "fields" (v9.6) package. For final visualization of the data, ggplot2 (v3.0.0) was used.

2.7 | Behavioral tests

For behavioral analysis, C57Bl6/JRj and CCR2$^{-/-}$ (males, 2.5–3 months old) were housed in groups of 2–5 animals in standard Typ II long filter top cages (Tecniplast, Germany) under specific pathogen free conditions with a 12/12 hr light–dark cycle. Mice underwent a standardized 4-weeks behavior training starting at 24 hr after single or repetitive injury, and were exposed to a set of behavioral tests which were conducted under standardized environmental conditions (humidity, temperature and light intensity). The same set of tests was repeated at 2 and 3 months past injury (mpi). Between individual testing phases animals were kept in familiar housing cages. Both handling and experimentation was carried out at the same time by the same person during the testing phases. AnyMaze Software (Stoelting Co.) and automated activity monitors were used to track the locomotor activity of mice and to analyze the data, if not stated otherwise.

Open field test (OF) was performed as previously described (Popper et al., 2018). In brief, for habituation in the test environment, mice were placed in the center of a 80 × 40 cm acrylic OF box at 1 dpi and were allowed to freely investigate the testing environment for 4 min. With a 24-hr delay, mice were re-tested in the OF for 4 min. For data analysis, the arena of the OF box was divided by the computer in two areas, the periphery defined as a corridor along the walls and the remaining area representing the center of the arena (see green color in representative track blots shown in Figures 5B and S7b). Locomotor activity (total distance, mean speed, the time and distance traveled in the center of the OF arena) was investigated using AnyMaze Software (Stoelting Co.). The first analysis (week 1) was carried out at 2 dpi.

Barnes maze assay (BM) was performed using the Barnes maze platform adapted to mice (Barnes, 1979), as previously described (Popper et al., 2018). In brief, all mice were placed in the center of the platform (starting point) for a total test duration of 4 min. The BM platform (Stoelting Europe, Ireland) consists of a circular surface (diameter 91 cm) with 20 circular holes (diameter 5 cm) around its circumference. The table surface is brightly lit by overhead lightning (900 lx), under one hole is a "flight box" (diameter 5 cm, depth 6 cm, length of the flight box: 15 cm). For each trial, the mice had 240 s to find the target zone and hide in the flight box. Recording was stopped either when the mouse entered the flight box or automatically after 240 s. One week before testing post injury, mice were trained in two trials per day (30 min interval) on four consecutive days (week 2). The test set up was not changed along the training phase. In the test phase, mice were exposed to the test set up once per day (24 hr interval) on four consecutive days (week 3). The location of the flight box was rotated by 90° in relation to the location in the training phase. The number of primary errors and the escape latency was determined during 240 s. The individual strategy to find the flight box (direct, wall, random) was analyzed by video tracking of all mice tested in the BM set up. No extra maze cues were used, and all surfaces were carefully cleaned with water after each individual.

2.8 | Statistical analysis

Statistical analysis of data was performed using PRISM (Graphpad, v5.03 and v7.0e). Appropriate statistical tests were chosen dependent on sample size, data distribution, and number of comparisons. The normality of distribution was analyzed using the Kolmogorov–Smirnov test or the Royston method of Shapiro–Wilk test. As indicated in figure legends, quantitative data are presented as mean ± *SEM*, mean ± *SD* or median ± interquartile range (IQR) with 25–75% range (borders) and 10–90% range (whiskers) of data distribution. All data consisting of two groups (e.g., WT mice after single vs. repetitive injuries) was analyzed with the non-parametric Wilcoxon-Mann–Whitney test. For multiple comparisons, differences were evaluated using one-way ANOVA followed by Tukey's multiple comparisons or non-parametric Dunn's post hoc test. To compare changes in proliferating astrocyte subsets between single and repeated injuries, the Welch *t* test of log2 fold differences was used. The minimum level of significance was defined as $p < .05$ and is indicated based on the *p*-value (*$p < .05$; **$p < .01$; ***$p < .001$).

3 | RESULTS

3.1 | Repetitive injury paradigm recruits new astrocytes into proliferation and causes some to divide repetitively

Given the cortical astrocyte heterogeneity at the morphological, functional, and molecular levels (Batiuk et al., 2020; Bayraktar et al., 2020; Khakh & Deneen, 2019; Lanjakornsiripan et al., 2018; Martin-Lopez, Garcia-Marques, Nunez-Llaves, & Lopez-Mascaraque, 2013; Westergard & Rothstein, 2020), we first asked if only a specific subset of parenchymal astrocytes can proliferate after TBI in the murine somatosensory cortex GM. To answer this, we performed repetitive injuries and used two different thymidine analogues, 5-bromo-2′-deoxyuridine (BrdU) and 5-ethynyl-2′-deoxyuridine (EdU) at different time periods after single or repetitive TBI (Figure 1A). First, we ensured the specificity of the antibody staining for BrdU in combination with the Click-iT EdU detection (see material and methods) and found highly selective and equal labeling efficiencies for each analog (Figure S1). We then applied BrdU for 10 days after TBI in the drinking water, paused by 4 days and followed by 10 days EdU application (Figure 1A). At the end of this labeling paradigm, that is, at 28 days post injury (dpi), reactive astrocytes were detected by immunolabelling for GFAP. Notably, within a 250 μm radius on each side of the injury core, virtually all astrocytes were GFAP$^+$, as determined by immunostaining for Aldh1L1-GFP (Figure S2). Approximately half of the astrocytes located within 250 μm on each side of the injury core
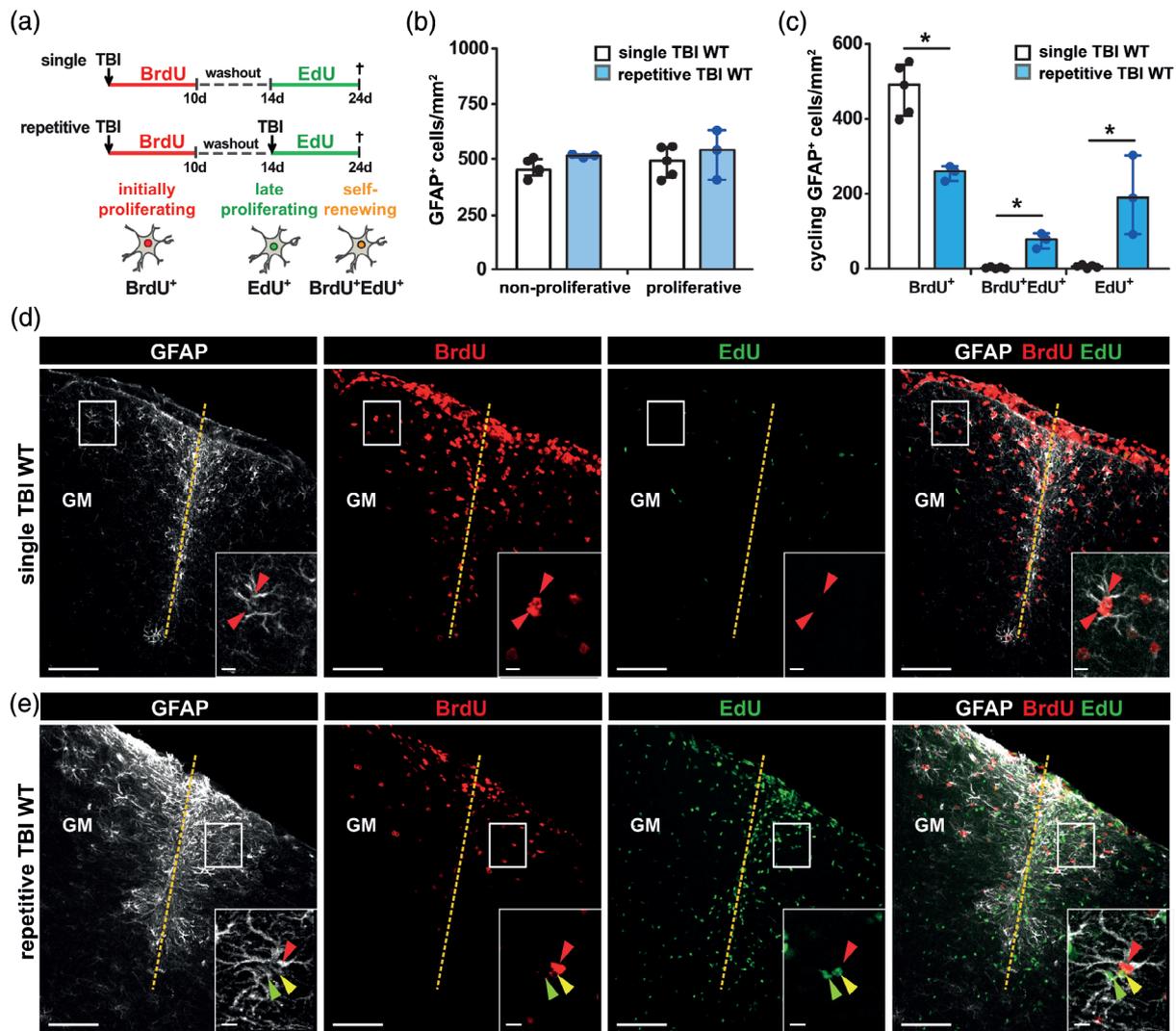
FIGURE 1 Upon repetitive injury parenchymal GM astrocytes divide repeatedly or new astrocytes enter proliferation in the second injury. Schematic outline of the analysis of astrocyte proliferation in response to single or repetitive TBI (a). The total number of reactive GFAP$^+$ cells at the injury site was comparable in both lesion conditions, and half of the reactive astrocytes incorporated proliferation markers in the vicinity of the lesion (b). Bar graph depicting proliferation of astrocytes after repetitive TBI in comparison to single TBI. The pool of proliferating astrocytes after repetitive injury consists of two subsets, newly dividing (EdU$^+$) and repeatedly dividing (BrdU$^+$/EdU$^+$) astrocytes (c). Representative immunostainings of BrdU and/or EdU labeled astrocytes at the site of single (d) or repetitive TBI (e). Insets depict examples of proliferating GFAP$^+$/BrdU$^+$ cells (red arrowheads), GFAP$^+$/EdU$^+$ cells (green arrowheads) and GFAP$^+$/BrdU$^+$/EdU$^+$ cells (yellow arrowheads). Data are depicted as median ± IQR with each dot representing one animal. Significance of differences between means is indicated based on the *p*-value (*$p < .05$; **$p < .01$; ***$p < .001$). Dashed yellow lines indicate the site of injury. GM: cerebral cortex grey matter. Scale bars: 100, 10 μm (insets)

had incorporated BrdU after a single lesion (Figure 1b), consistent with previous analysis (Buffo et al., 2008; Frik et al., 2018; Heimann et al., 2017; Heimann & Sirko, 2019; Sirko et al., 2013; Sirko et al., 2015). After a single injury, astrocyte proliferation was restricted within the first labelling period (BrdU) with no EdU$^+$ astrocytes detectable (Figure 1c,d), in agreement with our previous observations by live in vivo imaging (Bardehle et al., 2013). Interestingly, however, when a second injury of the same size was performed at the same location at 14 days after the first injury, many previously quiescent (not BrdU$^+$) astrocytes start to proliferate as one-third of all proliferating astrocytes was labeled by EdU only (Figure 1c,e). It became thus apparent that the injury-induced proliferative capacity is not

limited to the previously cycling subset of parenchymal astrocytes. Moreover, we also observed a significant number of BrdU/EdU double-positive astrocytes within the repetitively injured parenchyma (Figure 1c,e). To investigate whether both analogues have equal labeling efficiencies also after injury, we applied them together, and found indeed 93% BrdU$^+$/EdU$^+$ cells (Figure S3). Due to the short half-life of BrdU and its rapid clearance from the body (Barker, Charlier, Ball, & Balthazart, 2013) we could ensure that it would no longer be available after the 4 day washout period, and therefore we conclude that the BrdU$^+$/EdU$^+$ astrocytes after repetitive injury had divided following the first and also after second injury and hence are able to re-enter the cell cycle in vivo. These data demonstrate for the first time that

the proliferative reaction of astrocytes to repetitive injury consists of both newly and repeatedly proliferating astrocytes.

3.2 | Reactive astrocytes generate multicellular clones after repetitive injury

As cells may enter S-phase without completing cell division or incorporate DNA base analogs due to DNA damage (Taupin, 2007), we monitored the progeny of astrocytes at the single-cell level by clonal analysis using GLAST^{CreERT2}-mediated recombination in the multicolor R26-Confetti reporter mice (Bardehle et al., 2013; Calzolari et al., 2015) (Figure 2a,b). Application of low tamoxifen doses induced sparse astrocyte labelling across the uninjured brain. Consistent with the absence of astrocyte proliferation in the intact GM (Buffo et al., 2008; Sirko et al., 2009; Sirko et al., 2013), only single, non-proliferating astrocytes were observed in this region (Figure 2c,e).
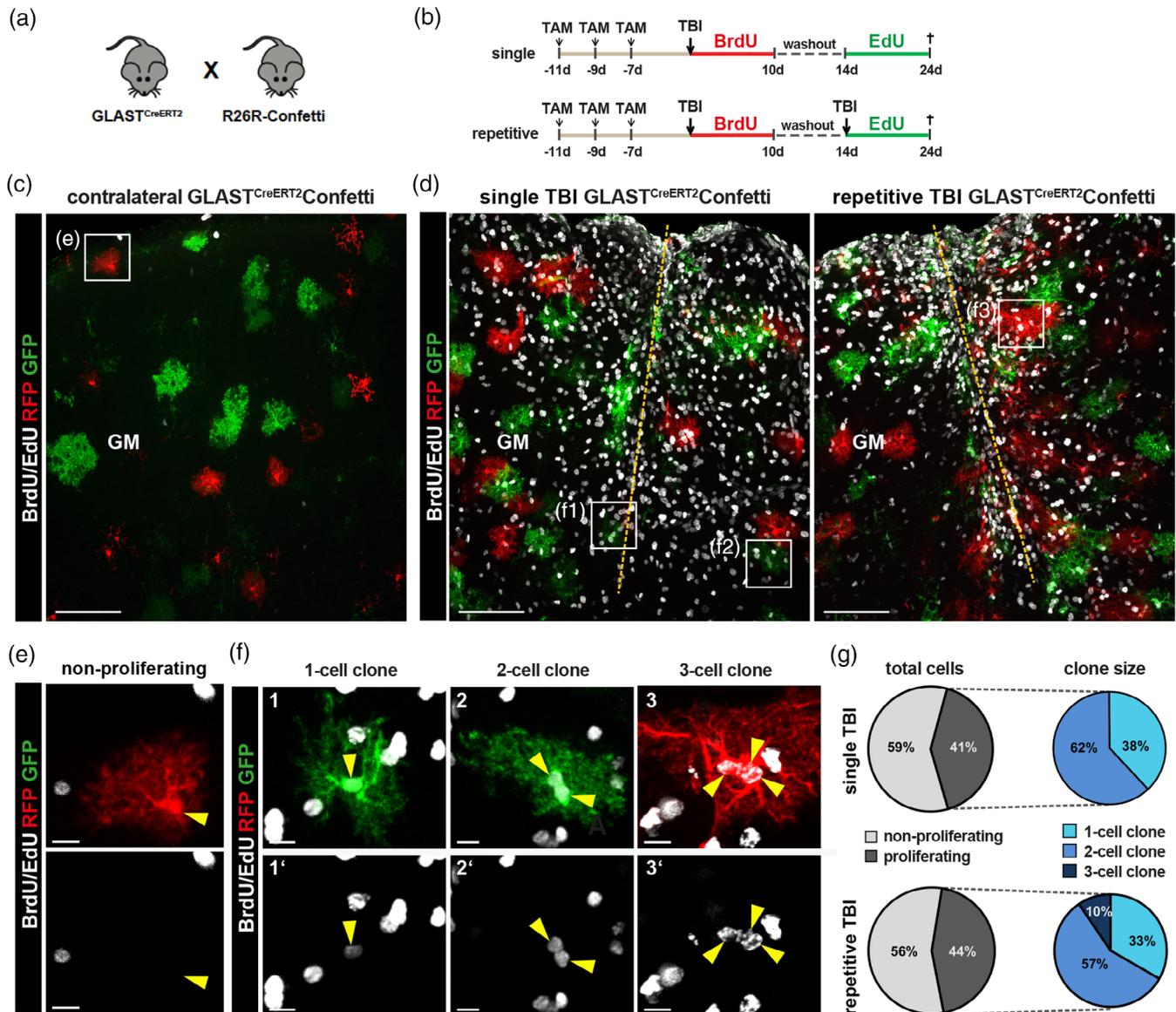

FIGURE 2 Reactive astrocytes within the injured GM parenchyma generate multicellular clones after injury. Clonal analysis was performed in GLAST^{CreERT2}Confetti mice (a). Schematic timeline of tamoxifen administration and injury time used for the analysis in GM GLAST^{CreERT2}Confetti mice (b). Representative photomicrograph of frontal brain section labeled for BrdU/EdU, RFP, and GFP displaying recombined cells in the contralateral (uninjured) (c), single and repeatedly injured GM of GLAST^{CreERT2}Confetti mice at 24 dpi (d). Higher magnifications of the GM areas indicated by the white boxes are shown in (e) and (f). Examples of non-proliferating RFP$^+$ astrocyte in the uninjured contralateral GM (e), as well 1-, 2-, and 3-cell clones (as indicated by yellow arrowheads) generated from single recombined astrocytes within the injured GM (f1–3) of GLAST^{CreERT2}Confetti mice. Pie charts illustrate the proportion of proliferating cells among all recombined astrocytes, and the clone size in the single and repeatedly injured GM of GLAST^{CreERT2}Confetti (g). Dashed yellow lines indicate the site of injury. GM: cerebral cortex grey matter. Scale bars: 100 μm (c–d), 10 μm (e, f)

In response to TBI, small clusters of GM astrocytes labeled in the same color were detected close to each other (Figure 2d,f), suggesting that these had arisen from a single proliferative cell to then form a multicellular clone. Importantly, half of all astrocytes labeled by fluorescent proteins had incorporated BrdU or EdU (Figure 2g), that is, the same proportion as determined above for GFAP$^+$ astrocytes. Thus, astrocytes labeled by GLAST^{CreERT2}-mediated tamoxifen induced recombination divide at the same rate as the total astrocyte population in WT animals. For the definition of multicellular clone, we measured 20 μm as the minimum distance between two cells with different fluorescent proteins (i.e., of different clonal origin) that had proliferated and incorporated thymidine analogues (Figure S4a,b). As a safe cut-off, we choose 5 μm (less than the diameter of astrocyte soma [Morel et al., 2019]) as the threshold distance for clonal origin, that is, cells expressing the same fluorescent protein derived from the same mother cell (Figure S4b). This very strict limit rather underestimates multicellular clones as false negatives, but ensures that we avoid "false positives," that is, clusters of cells interpreted as clones that are not derived from the same ancestor (Figure S4c,d). We decided for this strict cut-off also because our previous in vivo imaging analysis had shown that astrocytes that had divided upon injury stay very close together in most cases (Bardehle et al., 2013).

After a single injury, astrocyte duplets were often labeled with thymidine analogues (BrdU and/or EdU), indicating that they had not only incorporated DNA-base analogs indicative of S-phase, but had completed cell division and generated two daughter cells (Figure 2d,f). Most clones (62%) consisted of two daughter cells (Figure 2f,g), in agreement with previous live in vivo imaging observing mostly two daughter cells generated (Bardehle et al., 2013). However, a third of BrdU- or EdU-positive GLAST^{CreERT2}-labeled astrocytes were single cells (Figure 2g), suggesting incomplete cell cycle or death of a daughter cell. After repetitive injuries, we observed a few three-cell clones (Figure 2f,g), clearly indicating that a subset of reactive astrocytes can be activated to undergo a second division in vivo. As no larger clones were observed, it seems that self-renewal of reactive astrocytes is much more restricted than that of other glial cells, for example, the NG2 glia of the oligodendrocyte lineage or microglia (Jakel & Dimou, 2017; Tay et al., 2017).

3.3 | Alteration in astrocyte distribution after single and repetitive injury

The above results raise the question of how injury affects final astrocyte numbers and distribution. To determine this after single and repetitive TBI, we used Sox9 immunostaining (Figure S5) to label astrocyte nuclei (Sun et al., 2017) for unbiased automatic analysis of astrocyte numbers and their distribution at 28 dpi (Figure 3). Interestingly, we noted profound changes in astrocyte distribution compared to the contralateral uninjured cortex with a higher density in regions close to the injury site, shifting toward subpial positions after repetitive injury (Figure 3a). Despite the significant redistribution of astrocytes already after a single injury, there was no increase in the total number of

astrocytes quantified throughout the cortical thickness within 1 mm around the lesion site when compared with the same cortex region on the contralateral side (data not shown). After repetitive injuries, however, the total number of astrocytes and their density at the injury site were increased (Figure 3a). Given that astrocyte proliferation occurs predominantly at BV in this injury condition (Bardehle et al., 2013; Frik et al., 2018; Heimann et al., 2017), we aimed to determine the density of astrocytes in the BV vicinity and stained for the endothelial marker CD31 (Figures 3c and S6). Indeed, Sox9$^+$ cells significantly accumulated at CD31$^+$ BVs already after a single injury (Figure 3d). This was limited to 100 μm around the lesion core after one injury, but spread over several 100 μm after the second lesion (Figure 3d). Thus, TBI causes a severely altered distribution of astrocytes, with pronounced accumulation at the injury site and in the vicinity of BVs. This redistribution may have negative functional consequences given the key roles of astrocytes in information processing (Santello, Toni, & Volterra, 2019) or be beneficial shielding off more damaging agents.

3.4 | Monocyte infiltration promotes new astrocytes into proliferation causing further alterations in astrocyte distribution

Given that repetitive injury activates the same astrocytes to divide again and some astrocytes newly proliferate, we were interested to determine if this balance can be affected by extrinsic signals. As we had previously detected a potent influence of monocyte invasion on astroglia proliferation (Frik et al., 2018), we used CCR2$^{-/-}$ mice (Saederup et al., 2010) that entirely lack monocyte invasion into the injured brain parenchyma (Frik et al., 2018). Using the same experimental setting as described above (Figure 1a,b), we found that the absence of invading monocytes significantly enhanced cell cycle re-entry of astrocytes, resulting in a two-fold increase in the proportion of GFAP$^+$/BrdU$^+$/EdU$^+$ cells within the penumbra of repetitively injured CCR2$^{-/-}$ mice compared to WT (Figure 4a-c, Table 1). This substantially increased repetitive proliferation of reactive astrocytes was accompanied by reduced proliferation of previously quiescent astrocytes that incorporated only EdU after repetitive injuries in CCR2$^{-/-}$ mice compared to WT animals (Table 1). Thus, invading monocytes are crucial to inhibit re-entry of reactive astrocytes after repetitive injury.

This provided us with an experimental paradigm to explore, how the bias toward repetitive astrocyte divisions would affect their distribution after injury. Interestingly, the increased density of astrocytes shifted towards more superficial positions closer to the pial surface, already after one, but even more so after repetitive injury (Figure 3b). This could be explained by the penetrating injury from the pial surface with higher reactivity and astrocyte proliferation at upper positions (Sirko et al., 2009; Takata & Hirase, 2008) as well as the pial surface as main sites of monocyte invasion that would normally repress astrocyte proliferation (Frik et al., 2018). Likewise, the disbalance in astrocyte distribution with accumulation at the BVs was aggravated with significant increase at BVs even in the wider area of 1 mm already after a single injury (Figure 3e). Taken together, invading monocytes
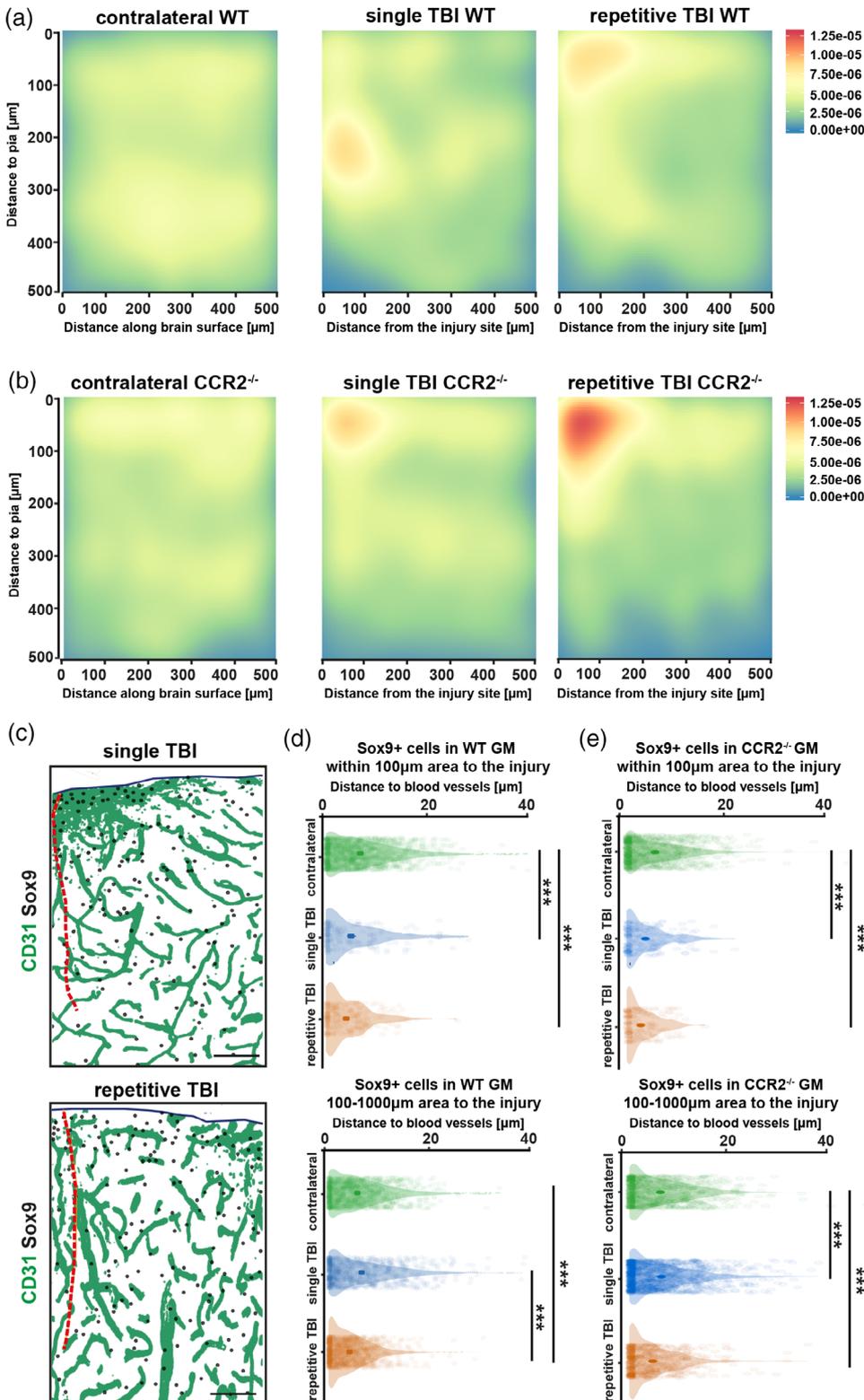
FIGURE 3 Injury-induced changes in distribution of astrocytes within the injured GM parenchyma. Immunolabelling of astrocytes (Sox9) was used for unbiased automatic analysis of astrocyte numbers and their distribution. Density plots depicting distribution of Sox9$^+$ astrocytes throughout the thickness of the uninjured contralateral GM and within parenchyma (in 500 μm radius) adjacent to the site of single or repetitive TBI in WT (a) and CCR2$^{-/-}$ (b) mice at 24 dpi. Automated analysis of astrocyte position relative to blood vessels was performed on frontal brain sections labeled with Sox9 and CD31. In order to get quantifiable binary pictures, the channels for CD31 and Sox9 were subjected to thresholding independently of each other using the Fiji inbuilt "Treshold"-function as shown in the black (Sox9$^+$)—green (CD31)—white panel (c). Violin plots show the distribution of Sox9$^+$ cells relative to CD31+ BVs in the uninjured contralateral GM as well as within 100 μm of the lesion core and more distal to it after single or repetitive TBI in the WT (d) and CCR2$^{-/-}$ (e) mice at 24 dpi. Data are depicted as mean ± *SEM*. Significance of differences between means is indicated based on the *p*-value (*p < .05; **p < .01; ***p < .001). Dashed red line indicates the site of injury, dark blue line indicates the pial border of the GM. GM: cerebral cortex grey matter. Scale bars: 120 μm (c)

inhibit further divisions of proliferating astrocytes rather promoting proliferation of additional astrocytes. This promotes the equal distribution of astrocytes postinjury. In the absence of invading monocytes, the disbalance in overall astrocyte distribution is aggravated, while, as previously shown, reactive astrocytes and scar formation are much reduced in the CCR2$^{-/-}$ mice after TBI (Frik et al., 2018).

3.5 | Behavioral analysis of functional recovery after injury

The above results provide intriguing entry points toward a better understanding of beneficial and adverse effects of astrocyte distribution for neurologic recovery. On the one hand, the homeostasis of
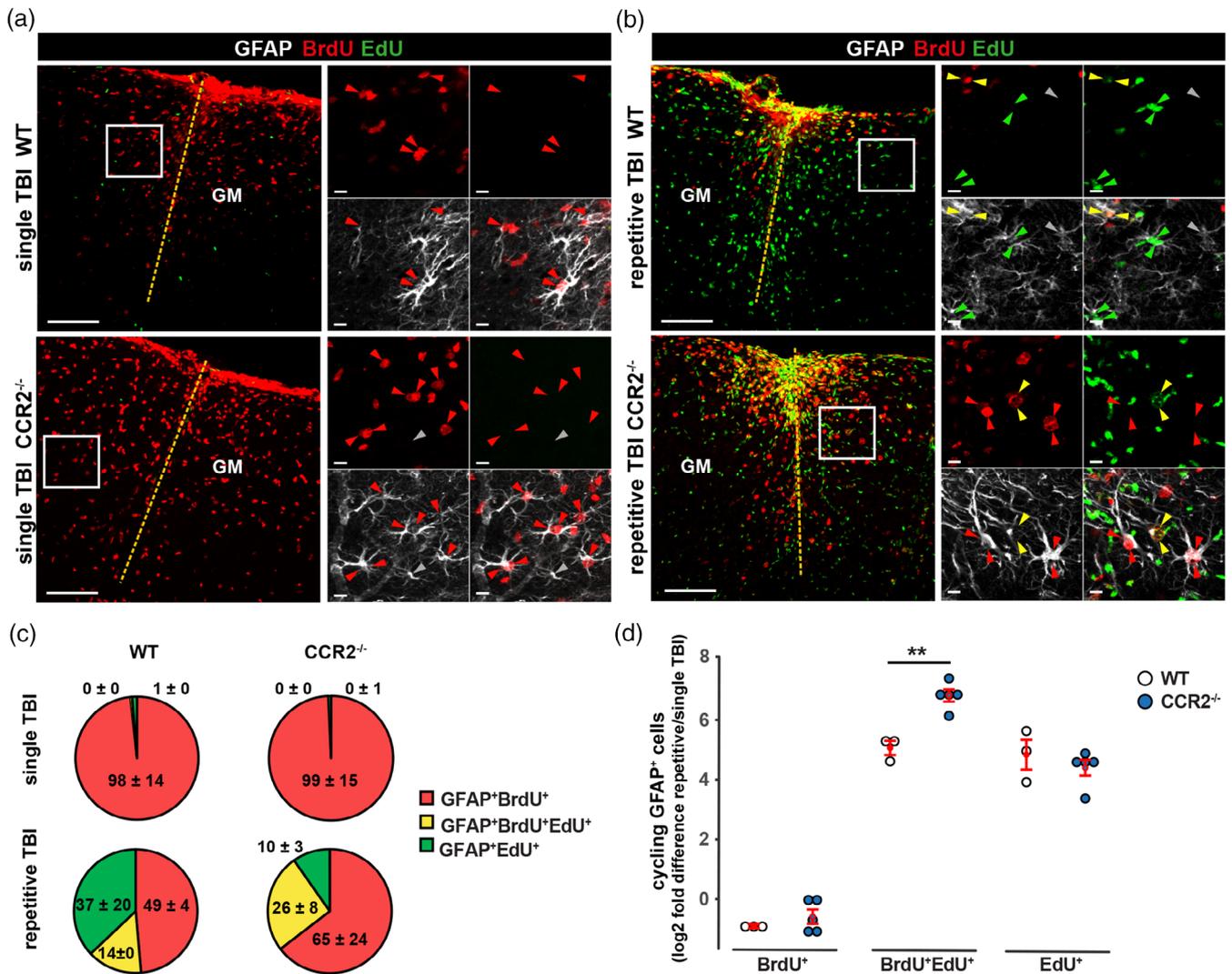
FIGURE 4 Astrocyte self-renewal within the injury-affected GM is modulated in the absence of infiltrating monocytes at the lesion area. Representative images displaying the regions of the WT and CCR2$^{-/-}$ somatosensory GM labelled for GFAP, BrdU and EdU after single (a) and repetitive TBI (b). Examples of proliferating GFAP$^+$/BrdU$^+$ cells (red arrowheads), GFAP$^+$/EdU$^+$ cells (green arrowheads) and GFAP$^+$/BrdU$^+$/EdU$^+$ cells (yellow arrowheads) are shown at higher magnifications. Pie charts illustrate the composition of the proliferating astrocyte pool in single and repeatedly injured GM of WT and CCR2$^{-/-}$ mice (c). The analysis of changes in proliferating astrocyte subsets between single and repeated injuries in WT and CCL2$^{-/-}$ mice revealed a significant genotype-related change in BrdU+EdU+ population following repetitive TBI in CCR2 versus WT mice (d). Data are depicted as mean ± *SEM* for dot plots (with each dot representing one animal) and mean ± *SD* for pie charts. Significance of differences between means is indicated based on the *p*-value (*$p < .05$; **$p < .01$; ***$p < .001$). Dashed yellow lines indicate the site of injury. GM: cerebral cortex grey matter. Scale bars: 100 μm, 10 μm (insets)

TABLE 1 Proliferating GFAP$^+$ cells across genotypes after single and repetitive injury

Number of cells (per mm^2)	Single TBI			Repetitive TBI		
	WT	CCR2$^{-/-}$	p	WT	CCR2$^{-/-}$	p
Proliferating GFAP$^+$	491.9 ± 137.1	547.1 ± 156.8	.1905	540.9 ± 224.8	522.8 ± 320.8	.7857
GFAP$^+$BrdU$^+$	490.5 ± 136.4	545.3 ± 150.1	.1111	259.6 ± 39.1	348.5 ± 287.8	.1429
GFAP$^+$BrdU$^+$ EdU$^+$	1.7 ± 4.7	0.9 ± 3.2	.7012	78.5 ± 40.4	156.6 ± 79.3	.0357
GFAP$^+$EdU$^+$	6.2 ± 8.7	1.8 ± 6.3	.3832	189.5 ± 210.4	64.1 ± 28.3	.0357

Note: The cell numbers are presented as median ± IQR (*n* = 3–5 per genotype/experimental group). Differences in the total numbers of proliferating GFAP$^+$ astrocytes and GFAP$^+$BrdU$^+$, GFAP$^+$EdU$^+$, or GFAP$^+$BrdU$^+$EdU$^+$ subpopulations of proliferating astrocytes between experimental animal groups are indicated by the *p*-value based on the non-parametric Wilcoxon-Mann–Whitney test.

astroglial numbers and distribution seems to be crucial for neural circuitry (Halassa & Haydon, 2010; Khakh & Sofroniew, 2015; Palpagama, Waldvogel, Faull, & Kwakowsky, 2019; Robel & Sontheimer, 2016; Siracusa, Fusco, & Cuzzocrea, 2019; van Dijk, Vergouwen, Kelfkens, Rinkel, & Hol, 2016; Verkhratsky & Zorec, 2019) and on the other hand accumulation of astrocytes may have beneficial effects by regulating inflammation (reducing monocyte invasion) and other harmful signals at sites where this is most needed. We therefore used well established tests for locomotion, such as the OF (Rodgers, Cao, Dalvi, & Holmes, 1997; Seibenhener & Wooten, 2015), and cognitive functions such as exploratory behavior, spatial memory and navigation by Barnes Maze (BM) (Bach, Hawkins, Osman, Kandel, & Mayford, 1995; Barnes, 1979; Van Den Herrewegen et al., 2019) (Figure 5). To exclude pre-existing differences between WT and CCR2$^{-/-}$ groups, we firstly performed behavioral evaluation of naïve CCR2$^{-/-}$ animals and found no significant differences between naïve WT and CCR2$^{-/-}$ animals throughout the duration of assessment (Figure S7).

WT mice showed significantly increased locomotor activity, measured as average speed and distance travelled in the OF, after both single and repetitive injury compared to uninjured (naïve) mice (Figure 5a). Such an increased activity was often observed in context with different types of brain injury and is indicative for increased risk-taking behavior (Laviola, Macri, Morley-Fletcher, & Adriani, 2003; Petraglia et al., 2014; Toledo-Rodriguez & Sandi, 2011). This is also reflected in the time spent in the center, as the natural tendency of rodents is to prefer darker areas along the walls (thigmotaxis) (Bailey & Crawley, 2009). WT mice showed increased risk taking with significantly more time spent in the center (Figure 5b,c). Strikingly, CCR2$^{-/-}$ mice showed no increase in locomotor activity (Figure 5a) and closely resembled the naïve mice at 3 months after single and already at 2 months after repetitive injury in regard to the risk-taking strategies (Figure 5b,c). Thus, CCR2$^{-/-}$ mice recover better from TBI compared with WT mice with no detectable differences at 3 months after single or repetitive TBI.

Similar trends were noted for the correction of injury-associated disturbances in spatial learning and memory. CCR2$^{-/-}$ mice showed significantly fewer primary errors in the BM compared with WT mice at 3 months after single and repetitive injury with no significant difference to the behavior of naïve mice (Figure 5d). Most pronounced differences were evident between WT and CCR2$^{-/-}$ mice when monitoring the strategy used in the BM. In search for the target hole, animals can use either a direct or focal path (used in 60–80% of naïve uninjured animals), or search along the walls/random walk, reflecting increased deficits in memory. Indeed, the latter behavior raises to over 50% on the training day in WT mice at 2 weeks postinjury and decreased to only little below 50% on the following test days (Figure 5e,f). Conversely, all injured CCR2$^{-/-}$ mice spend significant shorter time to reach the target hole by using either a focal or direct path to the hole on the relearning (test) day (Figure 5e,f). At 3 months after single TBI, WT mice still used in 50% of all cases the strategy to search along the walls, while CCR2$^{-/-}$ mice used the direct path in virtually all cases (Figure 5e,f). Strikingly, mice with repetitive injuries

performed generally better in this test with virtually all CCR2$^{-/-}$ mice using the direct paths strategy already at 2 months and WT at 3 months post injury (Figure 5f). These data show a correlation of conditions with increased astrocyte numbers and most pronounced changes in their distribution and better recovery in the behavior test—namely in CCR2$^{-/-}$ mice and after repetitive injury.

4 | DISCUSSION

Here we showed that the mode of astrocyte proliferation after TBI is subject to tight regulation with profound effects on the overall astrocyte distribution and density postinjury. Strikingly, invading monocytes inhibit—directly or indirectly—repetitive proliferation of astrocytes and rather favor proliferation of previously quiescent astrocytes upon repeated injury. This helps to distribute astrocytes more evenly, while repeated proliferation of the same astrocytes leads to higher accumulation at BVs and the injury site. The later seems, however, not to be deleterious as behavioral recovery was even enhanced in these conditions.

Despite the importance of astrocyte proliferation after injury, fundamental questions have remained previously answered, such as the extent of repeated astrocyte divisions, that is, their possible self-renewal and/or astrocyte subtype-specific proliferation. Here we showed that astrocyte proliferation is not restricted to the initially proliferating subset, as also previously quiescent astrocytes can be coerced to proliferate following repetitive TBI in the murine cerebral cortex GM. This was the case for ~30% of all proliferating astrocytes within the repeatedly injured GM area. We further provided clear evidence that reactive astrocytes can undergo several rounds of divisions in repetitive injury and that this proportion is significantly increased in CCR2$^{-/-}$ mice. This prompts the suggestion that astrocytes are able to self-renew, even though the exact identity of the clonally related astrocytes has not been determined. Notably, the ability of reactive astrocytes to self-renew was demonstrated so far only under neurosphere forming condition in vitro (Buffo et al., 2008; Sirko et al., 2009; Sirko et al., 2013). Most importantly, we assessed the consequences of these differential modes of astrocyte proliferation, repetitive or new astrocyte proliferation, on the post-traumatic astrocyte distribution and found a profound influence with higher accumulation at BVs and the injury site when more astrocytes divided repeatedly. This is intriguing, given the limited degree of astrocyte proliferation, compared to the much higher proliferation rates of microglia or NG2 glia (Jakel & Dimou, 2017; Nishiyama et al., 2016; Simon et al., 2011; Tay et al., 2017), but highlights the importance of the mechanisms regulating the proliferation of self-renewing or additional astrocyte populations.

One such mechanism is the invasion of monocytes, as their absence promoted proliferation of self-renewing versus newly recruited astrocytes. Indeed, many growth factors and extracellular matrix (ECM) factors are substantially altered after TBI in CCR2$^{-/-}$ mice (Frik et al., 2018; Kjell & Gotz, 2020) and could hence contribute to promote reactive astrocyte self-renewal. These were factors of
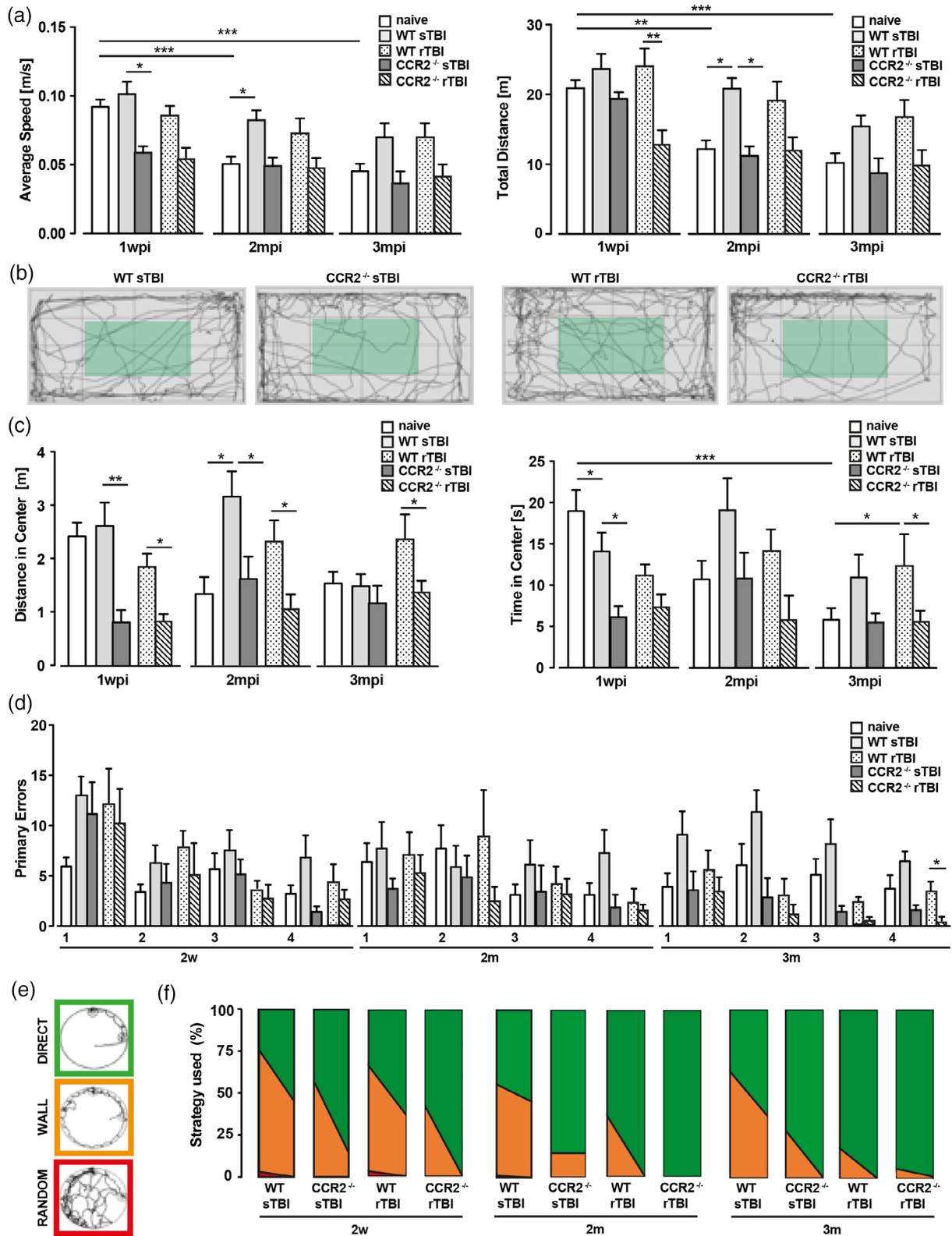
FIGURE 5 Legend on next page.

WNT, EGF, insulin/IGF and interleukin 3 signaling that have been implicated in regulating glial cell proliferation after injury (Dimou & Gotz, 2014; Gotz, Sirko, Beckers, & Irmler, 2015; Robel, Berninger, & Gotz, 2011). Furthermore, the absence of invading monocytes elicits not only the multiple effects on pathways regulating astrocyte proliferation at the lesion site, but also strongly affects ECM formation during acute and subacute stages after lesion (Frik et al., 2018; Kjell & Gotz, 2020). Given that many growth factors involved in the proliferative response at the injury site (e.g., FGF-2, VEGF, PDGF, TGF-β1) interact with the ECM (Brizzi, Tarone, & Defilippi, 2012; R. A. Clark, 2008; Hynes, 2009; Roll & Faissner, 2014), ECM changes observed in the injury site of the CCR2$^{-/-}$ mice (Frik et al., 2018; Kjell & Gotz, 2020) may modify the local concentration and/or ability of these factors to bind to their receptors, allowing a plethora of cell surface signaling pathways to influence astrocyte proliferation. Thus, monocyte invasion following TBI triggers many extrinsic factors promoting recruitment of new astrocytes into proliferation.

Importantly, the respective mode of astrocyte proliferation had profound effects on their post-traumatic distribution. We and others had previously described increased juxtavascular proliferation of reactive astrocytes resulting in the juxtavascular position of most (∼70%, see (Frik et al., 2018) newly generated astrocytes at the injury site (Bardehle et al., 2013; Frik et al., 2018; Jukkola, Guerrero, Gray, & Gu, 2013). We now show here that this resulted in a significantly lower distance of astrocytes to the BVs already after a single injury in WT mice, consistent with the lack of astrocyte migration in the cerebral cortex GM (Bardehle et al., 2013). This accumulation was spread even further within 1 mm surrounding of the injury site in CCR2$^{-/-}$ mice after a single injury, highlighting the importance of the mode of astrocyte divisions for their final posttraumatic distribution. This is important as the role of astrocytes in neurovascular coupling (for

review see, C. Y. Liu, Yang, Ju, Wang, & Zhang, 2018) may help to improve function at both the neurovascular and synaptic sites. Increased density of astrocytes in the vicinity of BVs helps stabilization of the BBB, the control of local microcirculation and cerebral blood flow within the perilesion area (Bylicky, Mueller, & Day, 2018; Chopp, Zhang, & Jiang, 2007; Faulkner et al., 2004; Frik et al., 2018; Heimann et al., 2017; Li et al., 2007; B. Liu, Teschemacher, & Kasparov, 2017; Ohab, Fleming, Blesch, & Carmichael, 2006; Takano et al., 2006). Accordingly, an injury-induced accumulation of astrocytes in vicinity of BVs is crucial for preventing secondary injury following TBI and may directly affect neuronal function and survival in the injury site (Robel & Sontheimer, 2016). This suggestion is further supported by the reduction of the NeuN-free area and an alleviated loss of synapses persisting in the injury site of CCR2$^{-/-}$ mice at the subacute phase after injury (Frik et al., 2018; Kjell & Gotz, 2020).

These improvements are likely to affect also synaptogenesis in the late phase after injury that is crucial for the functional outcome. It is noteworthy that reconfiguration of cortical circuitry occurs in a sequence of three phases after cortical injury (Biernaskie, Chernenko, & Corbett, 2004; Cramer & Riley, 2008; Ito, Kuroiwa, Nagasao, Kawakami, & Oyanagi, 2006; Kolb, Gibb, & Gorny, 2000; Murphy & Corbett, 2009; Nudo, Plautz, & Frost, 2001; Overman & Carmichael, 2014; Wieloch & Nikolich, 2006). In the acute injury phase, the cortex is challenged by a host of factors including cell death, inflammation, oxidative stress and loss of nutrients (Doyle, Simon, & Stenzel-Poore, 2008; Murphy & Corbett, 2009; Wieloch & Nikolich, 2006), which occur along with a loss of pyramidal cell dendritic spines (Zhang, Boyd, Delaney, & Murphy, 2005) and a rapid reduction in cortical inhibitory pathways for about 1–2 dpi (Chandrasekar et al., 2019; Imbrosci & Mittmann, 2011). This is beneficial as recently shown by chemogenic silencing of inhibitory neurons

FIGURE 5 Absence of invading monocytes at the injury site in CCR2$^{-/-}$ mice partially rescues hyperactivity and improves recovery of cognitive functions following injury in the somatosensory GM. The open field (OF) test was performed to assess spontaneous exploratory and anxiety-related behavior in novel/unfamiliar environment of WT and CCR2$^{-/-}$ mice at 1 day (1 wpi), 29 days (1 mpi) and 57 days (2 mpi) after single (sTBI) or repetitive injury (rTBI) (a–c). The injury-induced long-term hyperactivity of mice as shown by increased speed and total distance that WT mice traveled after single or repetitive TBI, compared with naïve controls. Lack of invading monocytes at the injury site in CCR2$^{-/-}$ mice reduced the levels of hyperactivity during acute and chronic phases after injury, compared with WT mice (a). Representative examples of movement path recorded in OF on second day after single or repetitive TBI in WT and CCR2$^{-/-}$ mice (b). The time and total distance traveled in center of the OF arena (indicated by green color in b) was recorded and analyzed at three time points after TBI. Graphs show statistical results for the effect of single and repetitive TBI on anxiety-related behavior of WT and CCR2$^{-/-}$ mice. Of note, CCR2$^{-/-}$ mice display enhanced anxiety only at 1 dpi as shown by reduced time spent and less distance moved in the center zone than naïve controls and injured WT mice. But in contrast to the injured WT, there were no sing of anxiety-related behavior of CCR2$^{-/-}$ mice during chronic phase after single or repetitive TBI (c). The Barnes maze (BM) was used to assess cognitive function, that is, spatial, hippocampus-dependent short- and long-term memory in WT and CCR2$^{-/-}$ mice at 2 w, 2 m, and 3 m after single and repetitive TBI. The mean number of errors before reaching the flight box was determined during 240 s in 2 trials per day on 4 consecutive days. Of note, while the numbers of primary errors/trials for the single and repetitively injured WT and CCR2$^{-/-}$ groups of animals were statistically identical during the first 8 weeks after TBI, the group CCR2$^{-/-}$ mice performed much better than the group of WT mice by making significantly less errors before reaching the flight box at 3 mpi (d). The individual strategy (direct, wall, random) to find the flight box rotated by 90° in relation to the location in the training phase was analyzed by video tracking of all mice tested in the BM set up (e). Graphs show the results for the effect of single and repetitive TBI as well as the significance of preventing monocyte invasion at the site of injury for hippocampus-dependent short-and long-term memory postinjury (f). Note that repeatedly injured WT mice performed better by locating the goal hole better than single injured WT animals. However, CCR2$^{-/-}$ mice in both injury groups equally demonstrated much improved recall of the goal location by using the direct strategy than injured WT mice. Data are depicted as mean ± SEM (WT mice/injury group: n = 11; CCR2$^{-/-}$ mice/injury group: n = 7; group of naïve animals: n = 15). Significance of differences between means is indicated based on the p-value (*p < .05; **p < .01; ***p < .001)

promoting pyramidal neuron survival after blunt TBI (Chandrasekar et al., 2019). Thus, the increase in neuronal excitation is beneficial (Domann, Hagemann, Kraemer, Freund, & Witte, 1993; Huemmeke, Eysel, & Mittmann, 2004; Imbrosci, Eysel, & Mittmann, 2010; Luhmann et al., 1996; Nahmani & Turrigiano, 2014; Qu, Mittmann, Luhmann, Schleicher, & Zilles, 1998), but critically depends on sufficient metabolic and homeostatic support from astrocytes to avoid further excitotoxicity. It is thus likely that the homeostatic re-adjustment of local astroglial networks may help to keep neuronal firing within a desirable range. Interestingly, transcriptome profiles of astrocytes isolated from the intact and the stab wounded somatosensory GM (Sirko et al., 2015) revealed that already at 5 dpi, astrocytes at the injury site normalized the expression of genes encoding for ion channels involved in the regulation of extracellular ion homeostasis (e.g., voltage-gated sodium and potassium channels as well as potassium inwardly-rectifying channels) to levels comparable to those in astrocytes from the intact GM of somatosensory cortex. Astrocytes maintain ionic and neurotransmitter homeostasis for example, by their large K^+ permeability and highly hyperpolarized membrane potential, and the expression levels of channels responsible for this (e.g., potassium inwardly-rectifying channel Kir4.1 (*Kcnj10*), the calcium-activated anion channel bestrophin1 (*Best1*), connexin 43 hemichannels, and the two-pore K^+ channel TWIK-1 (*KcnK6*) and TREK-1 (*KcnK2*)) have already normalized at this stage, eventhough normalizing protein levels may lag behind. Thus, the pronounced accumulation of astrocytes in upper cortical layers of the repeatedly injured somatosensory GM may be one of mechanisms helping to normalize circuit excitability, thereby promoting neuronal survival and functional recovery.

This interpretation lends support to the correlation that behavioral recovery occurs best in conditions with most pronounced astrocyte accumulation at BVs and in the upper cortex layers at the injury site. Here, we observed that the repeatedly injured WT and $CCR2^{-/-}$ mice exhibit not only reduced anxiety-like behavior, but also reduced injury-associated disturbances in spatial learning and memory during acute and chronic phases after injury, when compared with the single injured animals. As astrocyte number and distribution changed most in $CCR2^{-/-}$ mice and after repetitive injury, this may directly or indirectly contribute to the behavioral improvement via some of the mechanisms discussed above, or at least not be harmful. Behavioral and structural analysis has been performed using $CCR2^{-/-}$ mice in various injury conditions (Belarbi, Jopson, Arellano, Fike, & Rosi, 2013; Boring, Gosling, Cleary, & Charo, 1998; Clark et al., 2020; Hsieh et al., 2014; Izikson, Klein, Charo, Weiner, & Luster, 2000), but reactive astrogliosis and behavior were rarely examined in the same injury paradigm. Notably, the results of our behavioral tests are in line with previous studies demonstrating that blocking of monocyte infiltration by CCR2 inhibition or knockout can prevent spatial memory deficits and improve cognitive functions in different experimental models of TBI (Gyoneva et al., 2015; Hsieh et al., 2014; Liu et al., 2017; Morganti et al., 2015). The functional contribution of CCR2 to TBI pathology has been related to the overall reduced inflammatory state, smaller lesion size and decrease in the number of apoptotic cells and reactive astrogliosis as measured by GFAP immunoreactivity (Chu et al., 2014; Morganti et al., 2015). However, our previous study highlighted that the cross-regulation of juxtavascular proliferating astrocytes and invading monocytes is a crucial mechanism of scar formation upon brain injury (Frik et al., 2018). The results of our present study that self-renewal of astrocytes and their accumulation at BVs are favored in this condition add to highlight the key effects monocyte invasion has on final astrocyte distribution in addition to reduced scar formation and lesion size that may all contribute to better functional recovery. These observations are important because the primary damage of somatosensory cortex is among the most vulnerable targets in patients suffering TBI and causes neurobehavioral dysfunctions often resulting in long-persisting cognitive deficits (Maxwell, MacKinnon, Stewart, & Graham, 2010; Ouyang, Yan, Zhang, & Fan, 2017). Importantly, our work highlights the relevance to examine postinjury astrocyte distribution not exclusively by GFAP which only reveals astrocytes trapped in a reactive state (so far referred to as "scar"), but exploring the entire astrocyte population and their distribution that is highly relevant for neuronal circuit function and recovery. This is an important suggestion also for the analysis of human pathological samples to understand alterations in astrocyte distribution and density in patients.

CONFLICT OF INTEREST

The authors declare no competing interests.

DATA AVAILABILITY STATEMENT

The authors declare that the findings of this study are available in the article and in the supplementary material of this article. The data are available upon reasonable request from the corresponding authors.

ORCID

Magdalena Götz https://orcid.org/0000-0003-1551-9203
Swetlana Sirko https://orcid.org/0000-0001-5950-616X

REFERENCES

Anderson, M. A., Burda, J. E., Ren, Y., Ao, Y., O'Shea, T. M., Kawaguchi, R., ... Sofroniew, M. V. (2016). Astrocyte scar formation aids central nervous system axon regeneration. *Nature*, *532*(7598), 195–200. https://doi.org/10.1038/nature17623

Araque, A., Carmignoto, G., Haydon, P. G., Oliet, S. H., Robitaille, R., & Volterra, A. (2014). Gliotransmitters travel in time and space. *Neuron*, 81(4), 728–739. https://doi.org/10.1016/j.neuron.2014.02.007

Bach, M. E., Hawkins, R. D., Osman, M., Kandel, E. R., & Mayford, M. (1995). Impairment of spatial but not contextual memory in CaMKII mutant mice with a selective loss of hippocampal LTP in the range of the theta frequency. *Cell*, 81(6), 905–915. https://doi.org/10.1016/0092-8674(95)90010-1

Bailey, K. R., & Crawley, J. N. (2009). Anxiety-related behaviors in mice. In J. J. Buccafusco (Ed.), *Methods of behavior analysis in neuroscience* (2nd ed.). Boca Raton, FL: CRC Press/Taylor & Francis.

Bardehle, S., Kruger, M., Buggenthin, F., Schwausch, J., Ninkovic, J., Clevers, H., ... Gotz, M. (2013). Live imaging of astrocyte responses to acute injury reveals selective juxtavascular proliferation. *Nature Neuroscience*, 16(5), 580–586. https://doi.org/10.1038/nn.3371

Barker, J. M., Charlier, T. D., Ball, G. F., & Balthazart, J. (2013). A new method for in vitro detection of bromodeoxyuridine in serum: A proof of concept in a songbird species, the canary. *PLoS ONE*, 8(5), e63692. https://doi.org/10.1371/journal.pone.0063692

Barnes, C. A. (1979). Memory deficits associated with senescence: A neurophysiological and behavioral study in the rat. *Journal of Comparative and Physiological Psychology*, 93(1), 74–104. https://doi.org/10.1037/h0077579

Batiuk, M. Y., Martirosyan, A., Wahis, J., de Vin, F., Marneffe, C., Kusserow, C., ... Holt, M. G. (2020). Identification of region-specific astrocyte subtypes at single cell resolution. *Nature Communications*, 11(1), 1220. https://doi.org/10.1038/s41467-019-14198-8

Bayraktar, O. A., Bartels, T., Holmqvist, S., Kleshchevnikov, V., Martirosyan, A., Polioudakis, D., ... Rowitch, D. H. (2020). Astrocyte layers in the mammalian cerebral cortex revealed by a single-cell in situ transcriptomic map. *Nature Neuroscience*, 23(4), 500–509. https://doi.org/10.1038/s41593-020-0602-1

Belarbi, K., Jopson, T., Arellano, C., Fike, J. R., & Rosi, S. (2013). CCR2 deficiency prevents neuronal dysfunction and cognitive impairments induced by cranial irradiation. *Cancer Research*, 73(3), 1201–1210. https://doi.org/10.1158/0008-5472.CAN-12-2989

Ben Haim, L., & Rowitch, D. H. (2017). Functional diversity of astrocytes in neural circuit regulation. *Nature Reviews. Neuroscience*, 18(1), 31–41. https://doi.org/10.1038/nrn.2016.159

Biernaskie, J., Chernenko, G., & Corbett, D. (2004). Efficacy of rehabilitative experience declines with time after focal ischemic brain injury. *The Journal of Neuroscience*, 24(5), 1245–1254. https://doi.org/10.1523/JNEUROSCI.3834-03.2004

Boring, L., Gosling, J., Cleary, M., & Charo, I. F. (1998). Decreased lesion formation in CCR2$^{-/-}$ mice reveals a role for chemokines in the initiation of atherosclerosis. *Nature*, 394(6696), 894–897. https://doi.org/10.1038/29788

Brizzi, M. F., Tarone, G., & Defilippi, P. (2012). Extracellular matrix, integrins, and growth factors as tailors of the stem cell niche. *Current Opinion in Cell Biology*, 24(5), 645–651. https://doi.org/10.1016/j.ceb.2012.07.001

Buffo, A., Rite, I., Tripathi, P., Lepier, A., Colak, D., Horn, A. P., ... Gotz, M. (2008). Origin and progeny of reactive gliosis: A source of multipotent cells in the injured brain. *Proceedings of the National Academy of Sciences of the United States of America*, 105(9), 3581–3586. https://doi.org/10.1073/pnas.0709002105

Bylicky, M. A., Mueller, G. P., & Day, R. M. (2018). Mechanisms of endogenous Neuroprotective effects of astrocytes in brain injury. *Oxidative Medicine and Cellular Longevity*, 2018, 6501031. https://doi.org/10.1155/2018/6501031

Calzolari, F., Michel, J., Baumgart, E. V., Theis, F., Gotz, M., & Ninkovic, J. (2015). Fast clonal expansion and limited neural stem cell self-renewal in the adult subependymal zone. *Nature Neuroscience*, 18(4), 490–492. https://doi.org/10.1038/nn.3963

Chai, H., Diaz-Castro, B., Shigetomi, E., Monte, E., Octeau, J. C., Yu, X., ... Khakh, B. S. (2017). Neural circuit-specialized astrocytes: Transcriptomic, proteomic, morphological, and functional evidence. *Neuron*, 95(3), 531–549 e539. https://doi.org/10.1016/j.neuron.2017.06.029

Chandrasekar, A., Heuvel, F. O., Tar, L., Hagenston, A. M., Palmer, A., Linkus, B., ... Roselli, F. (2019). Parvalbumin interneurons shape neuronal vulnerability in blunt TBI. *Cerebral Cortex*, 29(6), 2701–2715. https://doi.org/10.1093/cercor/bhy139

Chopp, M., Zhang, Z. G., & Jiang, Q. (2007). Neurogenesis, angiogenesis, and MRI indices of functional recovery from stroke. *Stroke*, 38(2 Suppl), 827–831. https://doi.org/10.1161/01.STR.0000250235.80253.e9

Chu, H. X., Arumugam, T. V., Gelderblom, M., Magnus, T., Drummond, G. R., & Sobey, C. G. (2014). Role of CCR2 in inflammatory conditions of the central nervous system. *Journal of Cerebral Blood Flow and Metabolism*, 34(9), 1425–1429. https://doi.org/10.1038/jcbfm.2014.120

Clark, D., Brazina, S., Yang, F., Hu, D., Hsieh, C. L., Niemi, E. C., ... Marcucio, R. (2020). Age-related changes to macrophages are detrimental to fracture healing in mice. *Aging Cell*, 19(3), e13112. https://doi.org/10.1111/acel.13112

Clark, R. A. (2008). Synergistic signaling from extracellular matrix-growth factor complexes. *The Journal of Investigative Dermatology*, 128(6), 1354–1355. https://doi.org/10.1038/jid.2008.75

Cramer, S. C., & Riley, J. D. (2008). Neuroplasticity and brain repair after stroke. *Current Opinion in Neurology*, 21(1), 76–82. https://doi.org/10.1097/WCO.0b013e3282f36cb6

Dallerac, G., & Rouach, N. (2016). Astrocytes as new targets to improve cognitive functions. *Progress in Neurobiology*, 144, 48–67. https://doi.org/10.1016/j.pneurobio.2016.01.003

Dimou, L., & Gotz, M. (2014). Glial cells as progenitors and stem cells: New roles in the healthy and diseased brain. *Physiological Reviews*, 94(3), 709–737. https://doi.org/10.1152/physrev.00036.2013

Dimou, L., Simon, C., Kirchhoff, F., Takebayashi, H., & Gotz, M. (2008). Progeny of Olig2-expressing progenitors in the gray and white matter of the adult mouse cerebral cortex. *The Journal of Neuroscience*, 28(41), 10434–10442. https://doi.org/10.1523/JNEUROSCI.2831-08.2008

Domann, R., Hagemann, G., Kraemer, M., Freund, H. J., & Witte, O. W. (1993). Electrophysiological changes in the surrounding brain tissue of photochemically induced cortical infarcts in the rat. *Neuroscience Letters*, 155(1), 69–72. https://doi.org/10.1016/0304-3940(93)90675-b

Doyle, K. P., Simon, R. P., & Stenzel-Poore, M. P. (2008). Mechanisms of ischemic brain damage. *Neuropharmacology*, 55(3), 310–318. https://doi.org/10.1016/j.neuropharm.2008.01.005

Faiz, M., Sachewsky, N., Gascon, S., Bang, K. W., Morshead, C. M., & Nagy, A. (2015). Adult neural stem cells from the subventricular zone give rise to reactive astrocytes in the cortex after stroke. *Cell Stem Cell*, 17(5), 624–634. https://doi.org/10.1016/j.stem.2015.08.002

Faulkner, J. R., Herrmann, J. E., Woo, M. J., Tansey, K. E., Doan, N. B., & Sofroniew, M. V. (2004). Reactive astrocytes protect tissue and preserve function after spinal cord injury. *The Journal of Neuroscience*, 24(9), 2143–2155. https://doi.org/10.1523/JNEUROSCI.3547-03.2004

Frik, J., Merl-Pham, J., Plesnila, N., Mattugini, N., Kjell, J., Kraska, J., ... Gotz, M. (2018). Cross-talk between monocyte invasion and astrocyte proliferation regulates scarring in brain injury. *EMBO Reports*, 19(5), 20. https://doi.org/10.15252/embr.201745294

Gotz, M., Sirko, S., Beckers, J., & Irmler, M. (2015). Reactive astrocytes as neural stem or progenitor cells: in vivo lineage, in vitro potential, and genome-wide expression analysis. *GLIA*, 63(8), 1452–1468. https://doi.org/10.1002/glia.22850

Gyoneva, S., Kim, D., Katsumoto, A., Kokiko-Cochran, O. N., Lamb, B. T., & Ransohoff, R. M. (2015). Ccr2 deletion dissociates cavity size and tau pathology after mild traumatic brain injury. *Journal of Neuroinflammation*, 12, 228. https://doi.org/10.1186/s12974-015-0443-0

Halassa, M. M., & Haydon, P. G. (2010). Integrated brain circuits: Astrocytic networks modulate neuronal activity and behavior. *Annual Review of Physiology*, *72*, 335–355. https://doi.org/10.1146/annurev-physiol-021909-135843

Heimann, G., Canhos, L. L., Frik, J., Jager, G., Lepko, T., Ninkovic, J., ... Sirko, S. (2017). Changes in the proliferative program limit astrocyte homeostasis in the aged post-traumatic murine cerebral cortex. *Cerebral Cortex*, *27*(8), 4213–4228. https://doi.org/10.1093/cercor/bhx112

Heimann, G., & Sirko, S. (2019). Investigating age-related changes in proliferation and the cell division repertoire of parenchymal reactive astrocytes. *Methods in Molecular Biology*, *1938*, 277–292. https://doi.org/10.1007/978-1-4939-9068-9_20

Heintz, N. (2004). Gene expression nervous system atlas (GENSAT). *Nature Neuroscience*, *7*(5), 483. https://doi.org/10.1038/nn0504-483

Hirrlinger, J., Scheller, A., Hirrlinger, P. G., Kellert, B., Tang, W., Wehr, M. C., ... Kirchhoff, F. (2009). Split-cre complementation indicates coincident activity of different genes in vivo. *PLoS ONE*, *4*(1), e4286. https://doi.org/10.1371/journal.pone.0004286

Hol, E. M., & Pekny, M. (2015). Glial fibrillary acidic protein (GFAP) and the astrocyte intermediate filament system in diseases of the central nervous system. *Current Opinion in Cell Biology*, *32*, 121–130. https://doi.org/10.1016/j.ceb.2015.02.004

Hsieh, C. L., Niemi, E. C., Wang, S. H., Lee, C. C., Bingham, D., Zhang, J., ... Nakamura, M. C. (2014). CCR2 deficiency impairs macrophage infiltration and improves cognitive function after traumatic brain injury. *Journal of Neurotrauma*, *31*(20), 1677–1688. https://doi.org/10.1089/neu.2013.3252

Huemmeke, M., Eysel, U. T., & Mittmann, T. (2004). Lesion-induced enhancement of LTP in rat visual cortex is mediated by NMDA receptors containing the NR2B subunit. *The Journal of Physiology*, *559*(Pt 3), 875–882. https://doi.org/10.1113/jphysiol.2004.069534

Hynes, R. O. (2009). The extracellular matrix: Not just pretty fibrils. *Science*, *326*(5957), 1216–1219. https://doi.org/10.1126/science.1176009

Imbrosci, B., Eysel, U. T., & Mittmann, T. (2010). Metaplasticity of horizontal connections in the vicinity of focal laser lesions in rat visual cortex. *The Journal of Physiology*, *588*(Pt 23), 4695–4703. https://doi.org/10.1113/jphysiol.2010.198192

Imbrosci, B., & Mittmann, T. (2011). Functional consequences of the disturbances in the GABA-mediated inhibition induced by injuries in the cerebral cortex. *Neural Plasticity*, *2011*, 614329. https://doi.org/10.1155/2011/614329

Ito, U., Kuroiwa, T., Nagasao, J., Kawakami, E., & Oyanagi, K. (2006). Temporal profiles of axon terminals, synapses and spines in the ischemic penumbra of the cerebral cortex: Ultrastructure of neuronal remodeling. *Stroke*, *37*(8), 2134–2139. https://doi.org/10.1161/01.STR.0000231875.96714.b1

Izikson, L., Klein, R. S., Charo, I. F., Weiner, H. L., & Luster, A. D. (2000). Resistance to experimental autoimmune encephalomyelitis in mice lacking the CC chemokine receptor (CCR)2. *The Journal of Experimental Medicine*, *192*(7), 1075–1080. https://doi.org/10.1084/jem.192.7.1075

Jahn, H. M., Scheller, A., & Kirchhoff, F. (2015). Genetic control of astrocyte function in neural circuits. *Frontiers in Cellular Neuroscience*, *9*, 310. https://doi.org/10.3389/fncel.2015.00310

Jakel, S., & Dimou, L. (2017). Glial cells and their function in the adult brain: A journey through the history of their ablation. *Frontiers in Cellular Neuroscience*, *11*, 24. https://doi.org/10.3389/fncel.2017.00024

Jukkola, P., Guerrero, T., Gray, V., & Gu, C. (2013). Astrocytes differentially respond to inflammatory autoimmune insults and imbalances of neural activity. *Acta Neuropathologica Communications*, *1*, 70. https://doi.org/10.1186/2051-5960-1-70

Khakh, B. S., & Deneen, B. (2019). The emerging nature of astrocyte diversity. *Annual Review of Neuroscience*, *42*, 187–207. https://doi.org/10.1146/annurev-neuro-070918-050443

Khakh, B. S., & Sofroniew, M. V. (2015). Diversity of astrocyte functions and phenotypes in neural circuits. *Nature Neuroscience*, *18*(7), 942–952. https://doi.org/10.1038/nn.4043

Kjell, J., & Gotz, M. (2020). Filling the gaps - a call for comprehensive analysis of extracellular matrix of the glial scar in region- and injury-specific contexts. *Frontiers in Cellular Neuroscience*, *14*, 32. https://doi.org/10.3389/fncel.2020.00032

Kolb, B., Gibb, R., & Gorny, G. (2000). Cortical plasticity and the development of behavior after early frontal cortical injury. *Developmental Neuropsychology*, *18*(3), 423–444. https://doi.org/10.1207/S1532694208Kolb

Komitova, M., Zhu, X., Serwanski, D. R., & Nishiyama, A. (2009). NG2 cells are distinct from neurogenic cells in the postnatal mouse subventricular zone. *The Journal of Comparative Neurology*, *512*(5), 702–716. https://doi.org/10.1002/cne.21917

Lanjakornsiripan, D., Pior, B. J., Kawaguchi, D., Furutachi, S., Tahara, T., Katsuyama, Y., ... Gotoh, Y. (2018). Layer-specific morphological and molecular differences in neocortical astrocytes and their dependence on neuronal layers. *Nature Communications*, *9*(1), 1623. https://doi.org/10.1038/s41467-018-03940-3

Laviola, G., Macri, S., Morley-Fletcher, S., & Adriani, W. (2003). Risk-taking behavior in adolescent mice: Psychobiological determinants and early epigenetic influence. *Neuroscience and Biobehavioral Reviews*, *27*(1–2), 19–31. https://doi.org/10.1016/s0149-7634(03)00006-x

Li, L., Jiang, Q., Zhang, L., Ding, G., Gang Zhang, Z., Li, Q., ... Chopp, M. (2007). Angiogenesis and improved cerebral blood flow in the ischemic boundary area detected by MRI after administration of sildenafil to rats with embolic stroke. *Brain Research*, *1132*(1), 185–192. https://doi.org/10.1016/j.brainres.2006.10.098

Liu, B., Teschemacher, A. G., & Kasparov, S. (2017). Neuroprotective potential of astroglia. *Journal of Neuroscience Research*, *95*(11), 2126–2139. https://doi.org/10.1002/jnr.24140

Liu, C. Y., Yang, Y., Ju, W. N., Wang, X., & Zhang, H. L. (2018). Emerging roles of astrocytes in neuro-vascular unit and the tripartite synapse with emphasis on reactive gliosis in the context of Alzheimer's disease. *Frontiers in Cellular Neuroscience*, *12*, 193. https://doi.org/10.3389/fncel.2018.00193

Luhmann, H. J., Mittmann, T., Schmidt-Kastner, R., Eysel, U. T., Mudrick-Donnon, L. A., & Heinemann, U. (1996). Hyperexcitability after focal lesions and transient ischemia in rat neocortex. *Epilepsy Research. Supplement*, *12*, 119–128. Retrieved from https://www.ncbi.nlm.nih.gov/pubmed/9302510

Martin-Lopez, E., Garcia-Marques, J., Nunez-Llaves, R., & Lopez-Mascaraque, L. (2013). Clonal astrocytic response to cortical injury. *PLoS ONE*, *8*(9), e74039. https://doi.org/10.1371/journal.pone.0074039

Maxwell, W. L., MacKinnon, M. A., Stewart, J. E., & Graham, D. I. (2010). Stereology of cerebral cortex after traumatic brain injury matched to the Glasgow outcome score. *Brain*, *133*(Pt 1), 139–160. https://doi.org/10.1093/brain/awp264

Morel, L., Men, Y., Chiang, M. S. R., Tian, Y., Jin, S., Yelick, J., ... Yang, Y. (2019). Intracortical astrocyte subpopulations defined by astrocyte reporter mice in the adult brain. *GLIA*, *67*(1), 171–181. https://doi.org/10.1002/glia.23545

Morganti, J. M., Jopson, T. D., Liu, S., Riparip, L. K., Guandique, C. K., Gupta, N., ... Rosi, S. (2015). CCR2 antagonism alters brain macrophage polarization and ameliorates cognitive dysfunction induced by traumatic brain injury. *The Journal of Neuroscience*, *35*(2), 748–760. https://doi.org/10.1523/JNEUROSCI.2405-14.2015

Mori, T., Tanaka, K., Buffo, A., Wurst, W., Kuhn, R., & Gotz, M. (2006). Inducible gene deletion in astroglia and radial glia- -a valuable tool for

functional and lineage analysis. *GLIA*, *54*(1), 21–34. https://doi.org/10.1002/glia.20350

Murphy, T. H., & Corbett, D. (2009). Plasticity during stroke recovery: From synapse to behaviour. *Nature Reviews. Neuroscience*, *10*(12), 861–872. https://doi.org/10.1038/nrn2735

Nahmani, M., & Turrigiano, G. G. (2014). Adult cortical plasticity following injury: Recapitulation of critical period mechanisms? *Neuroscience*, *283*, 4–16. https://doi.org/10.1016/j.neuroscience.2014.04.029

Nishiyama, A., Boshans, L., Goncalves, C. M., Wegrzyn, J., & Patel, K. D. (2016). Lineage, fate, and fate potential of NG2-glia. *Brain Research*, *1638*, 116–128. https://doi.org/10.1016/j.brainres.2015.08.013

Nudo, R. J., Plautz, E. J., & Frost, S. B. (2001). Role of adaptive plasticity in recovery of function after damage to motor cortex. *Muscle & Nerve*, *24*(8), 1000–1019. https://doi.org/10.1002/mus.1104

Oberheim, N. A., Goldman, S. A., & Nedergaard, M. (2012). Heterogeneity of astrocytic form and function. *Methods in Molecular Biology*, *814*, 23–45. https://doi.org/10.1007/978-1-61779-452-0_3

Ohab, J. J., Fleming, S., Blesch, A., & Carmichael, S. T. (2006). A neurovascular niche for neurogenesis after stroke. *The Journal of Neuroscience*, *26*(50), 13007–13016. https://doi.org/10.1523/JNEUROSCI.4323-06.2006

Ouyang, W., Yan, Q., Zhang, Y., & Fan, Z. (2017). Moderate injury in motor-sensory cortex causes behavioral deficits accompanied by electrophysiological changes in mice adulthood. *PLoS ONE*, *12*(2), e0171976. https://doi.org/10.1371/journal.pone.0171976

Overman, J. J., & Carmichael, S. T. (2014). Plasticity in the injured brain: More than molecules matter. *The Neuroscientist*, *20*(1), 15–28. https://doi.org/10.1177/1073858413491146

Palpagama, T. H., Waldvogel, H. J., Faull, R. L. M., & Kwakowsky, A. (2019). The role of microglia and astrocytes in Huntington's disease. *Frontiers in Molecular Neuroscience*, *12*, 258. https://doi.org/10.3389/fnmol.2019.00258

Pekny, M., & Pekna, M. (2016). Reactive gliosis in the pathogenesis of CNS diseases. *Biochimica et Biophysica Acta*, *1862*(3), 483–491. https://doi.org/10.1016/j.bbadis.2015.11.014

Pekny, M., Wilhelmsson, U., Tatlisumak, T., & Pekna, M. (2019). Astrocyte activation and reactive gliosis-a new target in stroke? *Neuroscience Letters*, *689*, 45–55. https://doi.org/10.1016/j.neulet.2018.07.021

Petraglia, A. L., Plog, B. A., Dayawansa, S., Chen, M., Dashnaw, M. L., Czerniecka, K., ... Huang, J. H. (2014). The spectrum of neurobehavioral sequelae after repetitive mild traumatic brain injury: A novel mouse model of chronic traumatic encephalopathy. *Journal of Neurotrauma*, *31*(13), 1211–1224. https://doi.org/10.1089/neu.2013.3255

Popper, B., Demleitner, A., Bolivar, V. J., Kusek, G., Snyder-Keller, A., Schieweck, R., ... Kiebler, M. A. (2018). Staufen2 deficiency leads to impaired response to novelty in mice. *Neurobiology of Learning and Memory*, *150*, 107–115. https://doi.org/10.1016/j.nlm.2018.02.027

Qu, M., Mittmann, T., Luhmann, H. J., Schleicher, A., & Zilles, K. (1998). Long-term changes of ionotropic glutamate and GABA receptors after unilateral permanent focal cerebral ischemia in the mouse brain. *Neuroscience*, *85*(1), 29–43. https://doi.org/10.1016/s0306-4522(97)00656-8

Robel, S., Berninger, B., & Gotz, M. (2011). The stem cell potential of glia: Lessons from reactive gliosis. *Nature Reviews. Neuroscience*, *12*(2), 88–104. https://doi.org/10.1038/nrn2978

Robel, S., & Sontheimer, H. (2016). Glia as drivers of abnormal neuronal activity. *Nature Neuroscience*, *19*(1), 28–33. https://doi.org/10.1038/nn.4184

Rodgers, R. J., Cao, B. J., Dalvi, A., & Holmes, A. (1997). Animal models of anxiety: An ethological perspective. *Brazilian Journal of Medical and Biological Research*, *30*(3), 289–304. https://doi.org/10.1590/s0100-879x1997000300002

Roll, L., & Faissner, A. (2014). Influence of the extracellular matrix on endogenous and transplanted stem cells after brain damage. *Frontiers in Cellular Neuroscience*, *8*, 219. https://doi.org/10.3389/fncel.2014.00219

Saederup, N., Cardona, A. E., Croft, K., Mizutani, M., Cotleur, A. C., Tsou, C. L., ... Charo, I. F. (2010). Selective chemokine receptor usage by central nervous system myeloid cells in CCR2-red fluorescent protein knock-in mice. *PLoS ONE*, *5*(10), e13693. https://doi.org/10.1371/journal.pone.0013693

Santello, M., Toni, N., & Volterra, A. (2019). Astrocyte function from information processing to cognition and cognitive impairment. *Nature Neuroscience*, *22*(2), 154–166. https://doi.org/10.1038/s41593-018-0325-8

Seibenhener, M. L., & Wooten, M. C. (2015). Use of the open field maze to measure locomotor and anxiety-like behavior in mice. *Journal of Visualized Experiments*, *96*, e52434. https://doi.org/10.3791/52434

Simon, C., Gotz, M., & Dimou, L. (2011). Progenitors in the adult cerebral cortex: Cell cycle properties and regulation by physiological stimuli and injury. *GLIA*, *59*(6), 869–881. https://doi.org/10.1002/glia.21156

Siracusa, R., Fusco, R., & Cuzzocrea, S. (2019). Astrocytes: Role and functions in brain pathologies. *Frontiers in Pharmacology*, *10*, 1114. https://doi.org/10.3389/fphar.2019.01114

Sirko, S., Behrendt, G., Johansson, P. A., Tripathi, P., Costa, M., Bek, S., ... Gotz, M. (2013). Reactive glia in the injured brain acquire stem cell properties in response to sonic hedgehog. [corrected]. *Cell Stem Cell*, *12*(4), 426–439. https://doi.org/10.1016/j.stem.2013.01.019

Sirko, S., Irmler, M., Gascon, S., Bek, S., Schneider, S., Dimou, L., ... Gotz, M. (2015). Astrocyte reactivity after brain injury-: The role of galectins 1 and 3. *GLIA*, *63*(12), 2340–2361. https://doi.org/10.1002/glia.22898

Sirko, S., Neitz, A., Mittmann, T., Horvat-Brocker, A., von Holst, A., Eysel, U. T., & Faissner, A. (2009). Focal laser-lesions activate an endogenous population of neural stem/progenitor cells in the adult visual cortex. *Brain*, *132*(Pt 8), 2252–2264. https://doi.org/10.1093/brain/awp043

Snippert, H. J., van der Flier, L. G., Sato, T., van Es, J. H., van den Born, M., Kroon-Veenboer, C., ... Clevers, H. (2010). Intestinal crypt homeostasis results from neutral competition between symmetrically dividing Lgr5 stem cells. *Cell*, *143*(1), 134–144. https://doi.org/10.1016/j.cell.2010.09.016

Sun, W., Cornwell, A., Li, J., Peng, S., Osorio, M. J., Aalling, N., ... Nedergaard, M. (2017). SOX9 is an astrocyte-specific nuclear marker in the adult brain outside the neurogenic regions. *The Journal of Neuroscience*, *37*(17), 4493–4507. https://doi.org/10.1523/JNEUROSCI.3199-16.2017

Takano, T., Tian, G. F., Peng, W., Lou, N., Libionka, W., Han, X., & Nedergaard, M. (2006). Astrocyte-mediated control of cerebral blood flow. *Nature Neuroscience*, *9*(2), 260–267. https://doi.org/10.1038/nn1623

Takata, N., & Hirase, H. (2008). Cortical layer 1 and layer 2/3 astrocytes exhibit distinct calcium dynamics in vivo. *PLoS ONE*, *3*(6), e2525. https://doi.org/10.1371/journal.pone.0002525

Taupin, P. (2007). BrdU immunohistochemistry for studying adult neurogenesis: Paradigms, pitfalls, limitations, and validation. *Brain Research Reviews*, *53*(1), 198–214. https://doi.org/10.1016/j.brainresrev.2006.08.002

Tay, T. L., Mai, D., Dautzenberg, J., Fernandez-Klett, F., Lin, G., Sagar, ... Prinz, M. (2017). A new fate mapping system reveals context-dependent random or clonal expansion of microglia. *Nature Neuroscience*, *20*(6), 793–803. https://doi.org/10.1038/nn.4547

Toledo-Rodriguez, M., & Sandi, C. (2011). Stress during adolescence increases novelty seeking and risk-taking behavior in male and female rats. *Frontiers in Behavioral Neuroscience*, *5*, 17. https://doi.org/10.3389/fnbeh.2011.00017

Tripathi, R. B., Rivers, L. E., Young, K. M., Jamen, F., & Richardson, W. D. (2010). NG2 glia generate new oligodendrocytes but few astrocytes in a murine experimental autoimmune encephalomyelitis model of

demyelinating disease. *The Journal of Neuroscience, 30*(48), 16383–16390. https://doi.org/10.1523/JNEUROSCI.3411-10.2010

Van Den Herrewegen, Y., Denewet, L., Buckinx, A., Albertini, G., Van Eeckhaut, A., Smolders, I., & De Bundel, D. (2019). The Barnes maze task reveals specific impairment of spatial learning strategy in the Intrahippocampal Kainic acid model for temporal lobe epilepsy. *Neurochemical Research, 44*(3), 600–608. https://doi.org/10.1007/s11064-018-2610-z

van Dijk, B. J., Vergouwen, M. D., Kelfkens, M. M., Rinkel, G. J., & Hol, E. M. (2016). Glial cell response after aneurysmal subarachnoid hemorrhage - functional consequences and clinical implications. *Biochimica et Biophysica Acta, 1862*(3), 492–505. https://doi.org/10.1016/j.bbadis.2015.10.013

Verkhratsky, A., & Nedergaard, M. (2016). The homeostatic astroglia emerges from evolutionary specialization of neural cells. *Philosophical Transactions of the Royal Society of London. Series B, Biological Sciences, 371*(1700), 20150428. https://doi.org/10.1098/rstb.2015.0428

Verkhratsky, A., Rodriguez, J. J., & Parpura, V. (2014). Neuroglia in ageing and disease. *Cell and Tissue Research, 357*(2), 493–503. https://doi.org/10.1007/s00441-014-1814-z

Verkhratsky, A., & Zorec, R. (2019). Astroglial signalling in health and disease. *Neuroscience Letters, 689*, 1–4. https://doi.org/10.1016/j.neulet.2018.07.026

Wanner, I. B., Anderson, M. A., Song, B., Levine, J., Fernandez, A., Gray-Thompson, Z., ... Sofroniew, M. V. (2013). Glial scar borders are formed by newly proliferated, elongated astrocytes that interact to corral inflammatory and fibrotic cells via STAT3-dependent mechanisms after spinal cord injury. *The Journal of Neuroscience, 33*(31), 12870–12886. https://doi.org/10.1523/JNEUROSCI.2121-13.2013

Westergard, T., & Rothstein, J. D. (2020). Astrocyte diversity: Current insights and future directions. *Neurochemical Research, 45*, 1298–1305. https://doi.org/10.1007/s11064-020-02959-7

Wieloch, T., & Nikolich, K. (2006). Mechanisms of neural plasticity following brain injury. *Current Opinion in Neurobiology, 16*(3), 258–264. https://doi.org/10.1016/j.conb.2006.05.011

Wilhelmsson, U., Pozo-Rodrigalvarez, A., Kalm, M., de Pablo, Y., Widestrand, A., Pekna, M., & Pekny, M. (2019). The role of GFAP and vimentin in learning and memory. *Biological Chemistry, 400*(9), 1147–1156. https://doi.org/10.1515/hsz-2019-0199

Zawadzka, M., Rivers, L. E., Fancy, S. P., Zhao, C., Tripathi, R., Jamen, F., ... Franklin, R. J. (2010). CNS-resident glial progenitor/stem cells produce Schwann cells as well as oligodendrocytes during repair of CNS demyelination. *Cell Stem Cell, 6*(6), 578–590. https://doi.org/10.1016/j.stem.2010.04.002

Zhang, S., Boyd, J., Delaney, K., & Murphy, T. H. (2005). Rapid reversible changes in dendritic spine structure in vivo gated by the degree of ischemia. *The Journal of Neuroscience, 25*(22), 5333–5338. https://doi.org/10.1523/JNEUROSCI.1085-05.2005

Zhao, X., Ahram, A., Berman, R. F., Muizelaar, J. P., & Lyeth, B. G. (2003). Early loss of astrocytes after experimental traumatic brain injury. *GLIA, 44*(2), 140–152. https://doi.org/10.1002/glia.10283

SUPPORTING INFORMATION

Additional supporting information may be found online in the Supporting Information section at the end of this article.

How to cite this article: Lange Canhos L, Chen M, Falk S, et al. Repetitive injury and absence of monocytes promote astrocyte self-renewal and neurological recovery. *Glia*. 2020; 1–17. https://doi.org/10.1002/glia.23893